Novel Low-Cost Magnetic Clinoptilolite Powders/Granules for the Removal of Crystal Violet in Single and Binary Systems

Noori, Maryam; Tahmasebpoor, Maryam*+

Faculty of Chemical and Petroleum Engineering, University of Tabriz, Tabriz, I.R. IRAN

ABSTRACT: *Novel magnetic adsorbents of Clinoptilolite/Fe_3O_4 (Clin/Fe_3O_4) nanocomposite powders and Alginate/Clinoptilolite/Fe_3O_4 (Alg/Clin/Fe_3O_4) nanocomposite granules were synthesized to efficient removal of the cationic crystal violet (CV) dye in single and CV/methylene blue (MB) binary systems. The prepared adsorbents were characterized by FT-IR, XRD, SEM, EDX, dot mapping, and BET analysis. Adsorption tests showed that Clin/Fe_3O_4 and Alg/Clin/Fe_3O_4 had high affinity toward CV removal at 94.32% and 92.35%, in the single system and 84.19% and 80.23%, in the binary system, respectively. Based on the findings, pH was the most effective variable in the elimination process and the highest yield was obtained at pH 8 for both adsorbents. The equilibrium data followed the Langmuir model ($R^2 > 0.9$) based on which the maximum adsorption capacity (q_{max}) using Clin/Fe_3O_4 and Alg/Clin/Fe_3O_4 was determined as 44.662 mg/g and 16.528 mg/g, respectively in the single system and it was computed to be 15.797 mg/g and 11.476 mg/g, respectively in the binary system. The kinetic data fitted well to the pseudo-second-order model in both systems. The adsorption process was exothermic and thermodynamically spontaneous. Moreover, Clin/Fe_3O_4 and Alg/Clin/Fe_3O_4 adsorbents showed 91.43% and 82.01% recyclability over the desorption tests, thus leading to promising and green-based adsorbents for the removal of dyes. The Electrical Conductivity (EC) of MB, CV, and CV/MB solutions and also real wastewater sampled from a dyeing unit were measured before and after treatment and the results showed that the EC of all samples was reduced.*

KEYWORDS: *Crystal violet, Clinoptilolite, Granules, Binary system, Electrical conductivity.*

INTRODUCTION

Nowadays, water pollution due to the discharge of hazardous pollutants released from untreated or partially treated effluents of various industries into the water resources has caused great concerns worldwide because of its destructive effects on human health and the environment [1, 2]. Dyes are known as one of the main environmental pollutants in water sources, which are used in various chemical industries such as leather, textiles, plastics, rubber, paper, food, etc [3]. The presence of dyes in the water ambiance causes water pollution by increasing the toxicity, turbidity, and conductivity of colored effluents [3, 4]. In general, dyes are classified into three types cationic, anionic, and nonionic based on their structures, among them the toxicity of cationic dyes is

* *To whom correspondence should be addressed.*
+ E-mail: tahmasebpoor@tabrizu.ac.ir
1021-9986/2023/11/3601-3623 23/$/7.03

much higher than the others. Methylene Blue (MB) and Crystal Violet (CV) cationic organic dyes are most known for their widespread usage in the textile industry [5]. MB which is a non-biodegradable water-soluble dye cannot be decomposed for a long time due to its complex structure, and then causes harmful effects on aquatic ecosystems. Exposure to small amounts of MB dye leads to adverse effects such as increased heart rate, cyanosis, diarrhea, vomiting, jaundice, gastritis, respiratory problems, and chest pain in humans [6-8]. CV dye is toxic, mutagenic, carcinogenic, and mitotic in nature. Swallowing or inhaling CV dye can lead to gastrointestinal irritation, abdominal pain, pneumonia, peritonitis, skin or eye irritation, and birth defects. Also, the presence of CV dye in high concentrations in industrial effluents, can stop or reduce the oxygenation capacity of water and thus affect the biological activity and photosynthetic process of living organisms in the water [9]. Therefore, it is necessary to remove MB and CV dyes from industrial wastewater streams before entering the environment, due to the dangers and damages caused by the presence of these cationic dyes in aqueous solutions.

Various methods such as adsorption, electrochemical treatment, reverse osmosis, biological degradation, and chemical oxidation have been proposed to remove MB and CV toxic dyes from wastewater in various industries [10]. Among all the mentioned methods, adsorption seems to be the most effective, popularly adopted, and economically preferable technique to treat colored wastewater considering its cost-efficiency, not convoluted design process, high efficiency, and advantages in the case of non-toxic chemical reactions [11, 12]. Activated carbon has been proven to be an excellent adsorbent which is extensively studied among the other ones, but its high concern to activation, rapid saturation, and regeneration are substantial limitations known to researchers, prompting a search for alternative low-cost, eco-friendly, and effective adsorbents such as agricultural waste, fly ash, clay, rice husk, and zeolite [3, 13, 14].

Zeolites are highly porous aluminosilicates with a regular crystalline structure. Isomorphous substituting of Al^{+3} for Si^{+4} loads a negative charge on zeolites; this negative charge would be counterbalanced and neutralized by the cations, which can be exchanged with certain cations in the solution. Thus far, the number of globally recognized natural zeolites has exceeded 40. Clinoptilolite is contemplated as one of the naturally formed mineral zeolites which is frequently studied due to its abundance, low-cost, relatively high specific surface area, and high ion-exchange capacity. The above-mentioned properties make clinoptilolite a functional, effectual, and attractive choice of adsorbent for eliminating diverse and unwanted pollutants [15-18]. However, former researches have demonstrated that untreated clinoptilolite may not be regarded as an acceptable and satisfactory option for dye removal; which can be explained by its low capacity of adsorption [19]. Intending to enhance the adsorption capacity, chemical or thermal techniques can opt to modify the clinoptilolite. Modification of adsorbents using nanomaterials has gained considerable attention recently. The magnetic anoparticles may have several advantages, such as high adsorption capacity arising from their high specific surface area along with rapid and easy separation from the solutions because of their magnetic properties. In this regard, an efficient adsorbent with high capability in adsorbing pollutants from aqueous environments can be synthesized by modifying clinoptilolite using magnetic nanoparticles [20]. Although adsorbents modified with magnetic nanoparticles can be easily separated from aqueous media using an external magnet without the use of centrifugal or filtration processes, the use of powder-shape adsorbents is still limited in continuous systems due to the pressure drop occurred during the operation and also cracking of the powders [21, 22]. In addition, their adsorption capacity may plummet subsequently to the regeneration procedure. The mentioned disadvantages make powder adsorbents less attractive materials in large-scale water treatment processes. Therefore, the preparation of granules by using a suitable polymer matrix must be a promising method to resolve the mentioned drawbacks and increase the feasibility of powder adsorbents in wastewater treatment technologies [23]. Alginate (Alg) is a low-cost, non-toxic, and bio-degradable natural polysaccharide extracted from brown algae which has been applied as one of the most effective biological agents for the formation of powder/alginate composite granules due to its adsorption and gelling properties [12, 24, 25]. Using a suitable cross-linking agent like ferric chloride ($FeCl_3$), magnetic clinoptilolite can be immobilized within sodium alginate to be used as an adsorbent for treating the colored solutions.

Electrical Conductivity (EC) which is a measurement of the amount of electrical current a solution can carry, is considered one of the factors that represent the water quality.

This factor generally depends on the concentration of inorganic compounds such as nitrate, chloride, sulfate, and phosphate anions or calcium, magnesium, sodium, iron, and aluminum cations dissolved in the solution, usually measured as Total Dissolved Solids (TDS) [26]. The conductivity escalates as the ionic concentration soars, considering the fact that the electrical current is carried by ions in the solution. Hence, a significant change in the conductivity of a stream can be an indicator that a source of pollution has entered the stream [27]. The results reported in the literature showed a significant reduction of about 41.06 - 57.86% in EC of textile wastewater samples after treatment [28].

Despite a great number of literatures conducted on dyes removal from wastewater using various adsorbents, searching for the novel, low cost and innovative adsorbents with acceptable regenerability to achieve superior dye adsorption capacity still remains a controversial topic in the environmental field. Considering the comprehensive literature review, minor consideration has been paid to alginate granulated Clin/Fe_3O_4 nanocomposite adsorbents used for CV dye removal in binary systems. The main objective of this study is the identification of a low-cost adsorbent based on the most abundant natural zeolite in Iran; clinoptilolite, in the forms of both powders and granules for the removal of CV individually and in the presence of MB dye. It is worth stating that although previous works have not been focused on the industrial aspect of the adsorbents, the outcomes of this study revealed that the prepared granular Alg/Clin/Fe_3O_4 adsorbents could be used for industrial purposes due to their remarkable removal rate, cost-effective, and environmentally friendly properties. With the focus on the proposed purpose, first Fe_3O_4 magnetic nanoparticles are deposited on naturally-obtained clinoptilolite as the low-cost primary source. The synthesized Clin/Fe_3O_4 nanocomposite is then converted to Alg/Clin/Fe_3O_4 granules using a simple sodium alginate gelation method. The properties of the prepared adsorbents are characterized by various analyses such as SEM, EDX, XRD, VSM, BET, and FT-IR techniques. In an attempt to collate the adsorption efficiency of both powder and granule-shaped adsorbents, the adsorption of CV dye on Clin/Fe_3O_4 and Alg/Clin/Fe_3O_4 is probed and studied both in single and binary systems. Viable environment-related variables that could probably affect the adsorption process are optimized for both powder and granule-shaped adsorbents, such as pH, contact time, adsorbent dose, temperature, and initial concentration. The EC of the prepared CV and CV/MB solutions and also real wastewater is also measured before and after the adsorption process. Moreover, adsorption isotherms and kinetics of the removal process are studied based on the experimental data. The ability of Clin/Fe_3O_4 and Alg/Clin/Fe_3O_4 adsorbents to be reused for five cycles is also evaluated.

EXPERIMENTAL SECTION

Materials

Natural clinoptilolite ($AlCaH_6KNaO_3Si$) was provided from Mianeh's mountains located in East Azerbaijan of Iran and used as a raw material for synthesizing adsorbents. Crystal violet powder ($C_{25}H_{30}N_3Cl$, MW: 407.98 g/mol, λ_{max}:592 nm), methylene blue powder ($C16_6H_{18}N_3SCI$, MW: 319.85 g/mol, λ_{max}: 665 nm), iron (II) chloride ($FeCl_2$. $4H_2O$), iron (III) chloride ($FeCl_3$. $6H_2O$), hydrochloric acid (HCl), sodium hydroxide (NaOH), ethanol (C_2H_5OH), methanol (CH_3OH), potassium chloride (KCl), sodium chloride (NaCl), and calcium chloride ($CaCl_2$) were all supplied from Merck. Sodium alginate ($C_6H_7O_6Na$) was purchased from Sahand Shimi Co, Ltd., Iran. All chemicals were in analytical grade and used without any purification in this study. All experiments were operated using distilled water. The chemicals used in this research are listed in Table 1.

Adsorbents preparation

To produce Clin/Fe_3O_4 magnetic composite and Alg/Clin/Fe_3O_4 granules, co-precipitation, and ionic gelation methods were used based on previous studies [29, 30]. Briefly, the amount of 1.5 g of clinoptilolite was added to 250 mL of an aqueous solution containing Fe (III) and Fe (II) ions at a molar ratio of 2:1. While agitating by means of a magnetic stirrer, the mixture was set at 95°C for 40 min. Achieving a relatively higher pH, around 10, was ensured by the slow addition of NaOH (3 M, 50 mL). Subsequent to the finished stirring process, the obtained magnetic nanocomposites were successfully segregated from the solution with the help of a magnet. This step was followed by washing the produced adsorbents with distilled water several times until they were thoroughly neutralized. The mixture was finally put in an oven to dry at 110 °C for 24h and then ground by means of a miller. For the preparation of the Alg/Clin/Fe_3O_4 granules, 4g of alginate was first dispersed in 100 mL of distilled water under continuous stirring.

Table 1: List of chemicals used in this study

Chemical	Chemical formula	Abbreviation	Source
Natural clinoptilolite	$AlCaH_6KNaO_3Si$	Clin	Mianeh's mountains
Crystal violet powder	$C_{25}H_{30}N_3Cl$	CV	Merck
Methylene blue powder	$C1_6H_{18}N_3SCI$	MB	Merck
Iron (II) chloride	$FeCl_2.\ 4H_2O$	Fe (II)	Merck
Iron (III) chloride	$FeCl_3.\ 6H_2O$	Fe (III)	Merck
Hydrochloric acid	HCl	-	Merck
Sodium hydroxide	NaOH	-	Merck
Ethanol	C_2H_5OH	-	Merck
Methanol	CH_3OH	-	Merck
Potassium chloride	KCl	-	Merck
Sodium chloride	NaCl	-	Merck
Calcium chloride	$CaCl_2$	-	Merck
Sodium alginate	$C_6H_7O_6Na$	Alg	Sahand Shimi

After reaching a homogeneous mixture, a certain amount of Clin/ Fe_3O_4 powder, with alginate to Clin/Fe_3O_4 ratio of 1/4 was added to the alginate suspension. Then, it was dropped slowly by syringe into an aqueous solution containing $FeCl_3$ solution (2% w/v, 100 mL) in order to the formation of the granules. The provided round-shaped granules were kept in $FeCl_3$ solution overnight until the completion of the gelation process. Finally, after being separated, the granules were washed several times utilizing distilled water, so as to remove residues of Fe ions on the surface, and then dried in a hot oven at 55°C. Fig. 1 shows an overview of the Clin/Fe_3O_4 and Alg/Clin/Fe_3O_4 synthesis processes.

Solutions

The initial stock solution of CV was prepared by dissolving 1g dye in 1000 mL distilled water. For the binary CV/MB aqueous solution system, a 1:1 dye concentration ratio was used. Each solution with the required initial concentration was arranged by diluting the stock solution.

Adsorbents characterization

The prepared Clin/Fe_3O_4 composite and Alg/Clin/Fe_3O_4 granules were characterized by scanning electron microscope (SEM, MIRA3 FEG-SEM, Tescan), X-ray diffraction (XRD, Siemens D500), Brunauer-Emmett-Teller (BET, BELSORP MINI II), and energy-dispersive X-ray spectrometer (EDX) methods. The Fourier Transform Infrared (FT-IR) (Bruker, Tensor 27 spectrometer) with the wavenumber ranging 400–4000 cm^{-1} was employed intending to detect the surface functional groups. The magnetic properties of Clin/Fe_3O_4 and Alg/Clin/ Fe_3O_4 were studied on a vibrating sample magnetometer (VSM, MPMS-5 SQUID). The concentration of CV was determined at the proper wavelength using UV–Visible spectrophotometer (Analytik Jena, Specord250) considering the calibration curve acquired from first-order derivatives of the spectra. The electric conductivity of the samples was measured with an AZ 86503 conductivity meter. The adjustment of pH values was made possible in the range of 2 to 12 by the addition of HCl or NaOH solutions using pH-meter Adwa AD1020.

Adsorption experiments

The batch-mode experiments were performed for the adsorption process of CV in a single and CV/MB binary mixture from an aqueous environment by Clin/Fe_3O_4 composite and Alg/Clin/Fe_3O_4 granules. The effect of the environment-related parameters including pH (ranging from 2 to 12), contact time (between 5 and 120 min), adsorbent dose (ranging from 0.5 to 3 g/L), temperature (between 25 and 45 °C), and dye concentration (ranging from 10 to 50 mg/L) was explored on the adsorption process. With the aim of investigating the effect of the pH of the solution on the adsorption performance, the experiments were carried out at pH in the range of 2-12 and fixed other laboratory conditions such as an adsorbent dose of 1 g/L, contact time of 60 min, the temperature of 25°C, and initial dye concentration of 10 mg/L. After adjusting the optimal pH, other influential variables such as

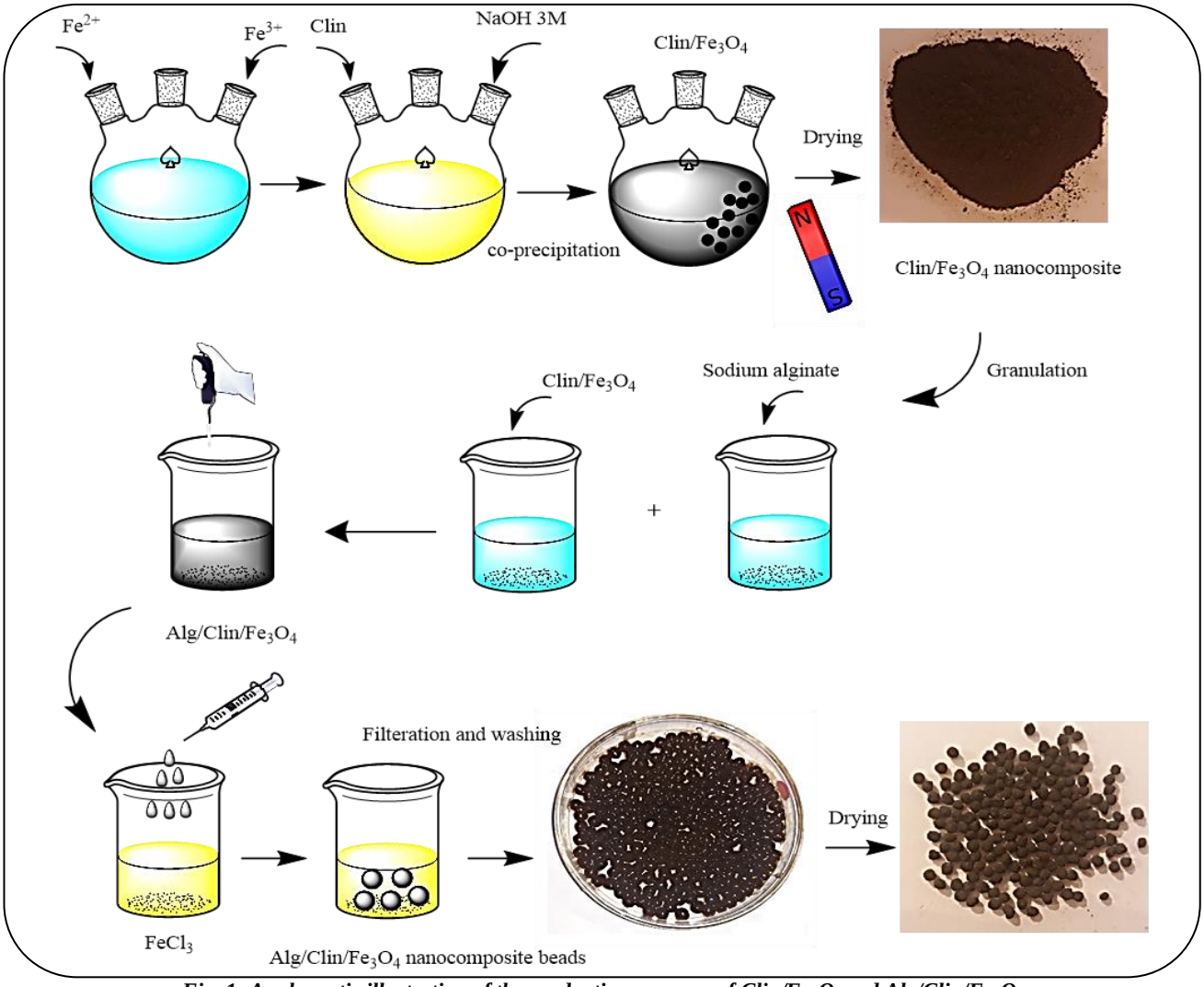

Fig. 1: A schematic illustration of the productions process of Clin/Fe3O4 and Alg/Clin/Fe3O4

as contact time, initial concentration of dyes, adsorbent dose, and temperature were studied. The adsorption capacity (q_e, mg/g) and removal percentage (R %) for all samples were computed using Eq. (1) and (2), respectively.

$$R\% = \frac{C_o - C_e}{C_o} \times 100 \quad (1)$$

$$q_e = \frac{(C_o - C_e) \times V}{M} \quad (2)$$

C_o indicates the initial concentration of dye (mg/L), while C_e designates the equilibrium concentration of dye (mg/L). The mass of the adsorbent (g) is signified by M and V stands for the volume of the dye solution (L) [31].

Desorption and Regeneration

The desorption of CV from $Clin/Fe_3O_4$ composite and $Alg/Clin/Fe_3O_4$ granules was performed in 10 mL of diverse solutions which includes ethanol, methanol, 0.1M HCl, 0.5M NaCl, 0.5M KCl, and ethanol + 0.5M $CaCl_2$ under magnetic stirring for 4 h. From the mentioned solutions, the one with the highest desorption percentage was favored and picked as the desorption solution, hence further experiments were carried out in the determined solution. In an attempt to enhance the desorption percentage in the preferred solution, the residence time in the chosen solution was expanded to 24h. Thereafter, regenerated adsorbents were washed comprehensively with deionized water, after which they were dried in the oven. In order to study the possibility of reusability, a certain amount of regenerated adsorbent was mixed with 100 mL of CV and CV/ MB mixture (10 mg/L). The aforementioned cycle of adsorption-desorption was repeated for five rounds, during which the amount of either

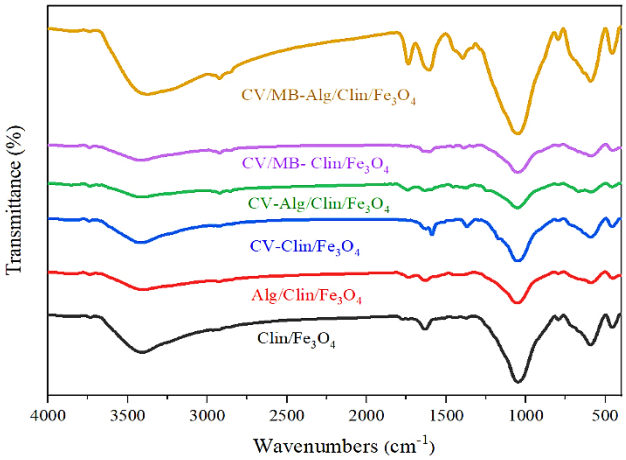

Fig. 2: FT-IR spectra of Clin/Fe3O4 and Alg/Clin/Fe3O4 before and after CV dye adsorption in single and binary systems

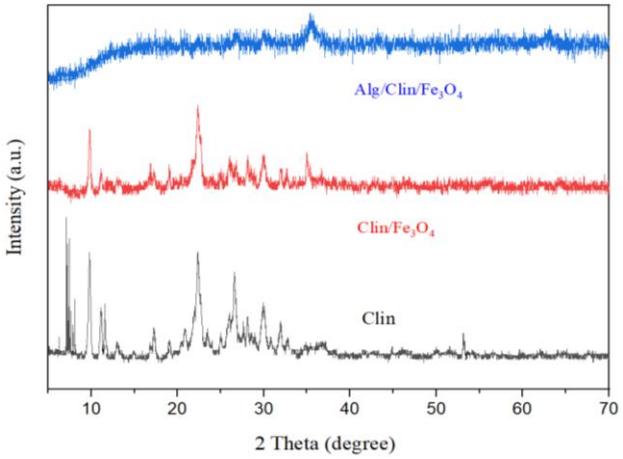

Fig. 3: XRD patterns of clinoptilolite, Clin/Fe3O4 and Alg/Cline/Fe3O4

adsorbed or desorbed dye was measured by spectrophotometer. The calculation of the desorbed amount of dye was made possible by Eq. (3) [32].

$$\text{Desorption} = \left(\frac{C_m}{C_e}\right) \times 100 \quad (3)$$

C_m represents the released dye concentration in the solution, and C_e defines the concentration of dye which was adsorbed initially.

Electrical conductivity (EC) measurement

Solutions of MB and CV dyes individually and also a binary system of CV/MB mixture with concentrations of 10 mg/L were prepared. Real wastewater was sampled from the Valizadeh dyeing unit located in East Azerbaijan, Iran. In order to investigate the applicability of the adsorbents in decreasing the electrical conductivity, the EC of the samples was measured with a digital conductivity meter before and after the adsorption process.

RESULTS AND DISCUSSION

Characterization of the adsorbents

The FT-IR technique opted in order to look into the effective functional groups present in the structure of Clin/Fe_3O_4 and Alg/Clin/Fe_3O_4 adsorbents before and after CV dye adsorption. The FT-IR results are represented in Fig. 2. The sharpest band at around 1048 cm^{-1} corresponded to the asymmetric vibrations of Si-O-Si and Si -O-Al [33]. C-H, O-H, and, H-OH stretching in the structure of the adsorbents was associated with the detected bands in the ranges of 2923-2926 cm^{-1}, 3413-3421 cm-1, and 1629-1632 cm^{-1}, respectively [34]. Moreover, the deposition of Fe_3O_4 on the surface of clinoptilolite in both Clin/Fe_3O_4 and Alg/Clin/Fe_3O_4 adsorbents can be considered affirmative. This confirmation is considered valid due to the vibrational bands which appeared at 592 cm^{-1} and 589 cm^{-1} associated with Fe-O [35]. In the case of Alg/Clin/Fe_3O_4, the detected peak at 3678 cm^{-1} might be connected to C-H rings, which are considered aromatic, inside the alginate's structure. Furthermore, the peak located at 1736 cm^{-1} can be ascribed to the vibrations of carboxyl and amidic carbonyl groups. [36]. After adsorbing CV and MB cationic dyes with the adsorbents, some changes in the positions of the peaks appeared, which could be on the grounds of the interactions between the active functional groups of the adsorbents and dye molecules. For example, newfound peaks are detected within the structure of Alg/Clin/Fe_3O_4 at 1374 cm^{-1} after the adsorption of CV molecules. This phenomenon can be explained by the bending vibrations of the C-H group, which is due to CH_2 or CH_3 [37]. Additionally, the latest vibrational bands seen at 1330 cm^{-1} after CV/MB adsorption by Clin/Fe_3O_4 can be attributed to the bending mode of the CH and the twisting mode of the $-CH_2-$ group [38].

The XRD analysis was implemented to investigate the crystalline structure of clinoptilolite, Clin/Fe_3O_4 and, Alg/Clin/Fe_3O_4, and the results are presented in Fig. 3. The peaks observed at angles around 2θ= 22°, 26°, 28°, and 29° for natural clinoptilolite are all well consistent with its XRD data reference (JCPDS # 39-1383) [39]. New peaks observed at 2θ values around 30°, 35°, 43°, 56° and 63°, in the XRD pattern of Clin/Fe_3O_4 are related to Fe_3O_4

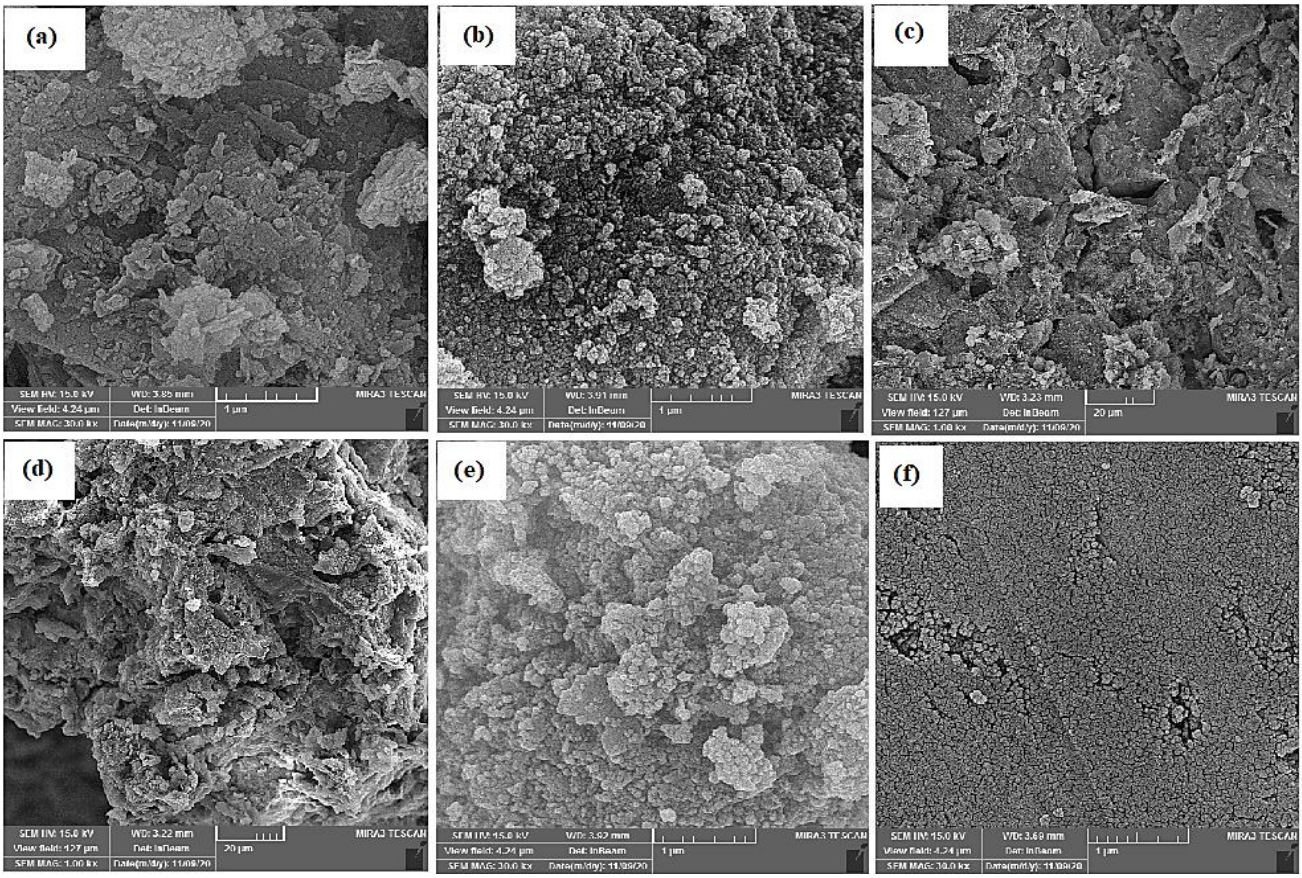

Fig. 4: SEM analysis micrographs obtained for (a) natural clinoptilolite, (b) Clin /Fe_3O_4, (c) external surface of Alg/Clin/Fe_3O_4 (d) inner surface of Alg/Clin/Fe_3O_4, (e) Clin/Fe_3O_4 after CV dye adsorption, (f) Alg/Clin/Fe_3O_4 after CV dye adsorption

nanoparticles [29]. Collating the intensities of the peaks, which are normally corresponded to the crystallinity of the structures, relies on the poorly crystalline structure of Alg/Clin/Fe_3O_4 in comparison with Clin/Fe_3O_4. Alginate molecules in the Alg/Clin/Fe_3O_4 adsorbent's structure may be the feasible explanation for peaks with weaker intensities in the XRD pattern [36]. In addition, XRD analysis cannot be a desirable and satisfactory method to adopt when it comes to polymeric components such as alginate [29].

The SEM images taken from natural clinoptilolite, Clin/Fe_3O_4, and Alg/Clin/Fe_3O_4 (prior and following to CV dye adsorption) are demonstrated in Fig. 4. It can be observed that the natural clinoptilolite has an anomalous, particularly rough, and layered crystalline structure, however, the roughness is considerably less declared for Clin/Fe_3O_4 (Fig. 4a and 4b). The pictures taken from the inner (Fig. 4c) and outer (Fig. 4d) surfaces of Alg/Clin/Fe_3O_4 adsorbent confirm the formation of an entirely porous structure including Clin/Fe_3O_4 and alginate's network after adsorbents granulated. After the adsorption of CV dye on Clin/Fe_3O_4, and Alg/Clin/Fe_3O_4, some changes were made in both adsorbent's surfaces (please see Figs. 4e and 4f), which can be attributed to the viable placement of dye molecules in the layers and pores of the powder and granules. Therefore, it can be concluded that these adsorbents have an effective ability to adsorb the CV dye from aqueous media.

EDX and mapping analysis was also used to determine the density and distribution of elements in the structure of Clin/Fe_3O_4. The results showed that in the structure of Clin/Fe_3O_4, in addition to the basic elements, Fe (52.24%) and O (33.38%) elements are also present, which is definitely caused by Fe_3O_4 magnetic nanoparticles (Fig. 5).

With the aim of determining the magnetic characteristics of Clin/Fe_3O_4 and Alg/Clin/Fe_3O_4, VSM analysis was carried out. The magnetic saturation values of 14.107 emu/g and 12.658 emu/g were measured for Clin/Fe_3O_4 and Alg/Clin/Fe_3O_4, respectively. As it can be seen, the amount of magnetic saturation for Clin/Fe_3O_4 is higher than that for Alg/Clin/Fe_3O_4, this differentiation

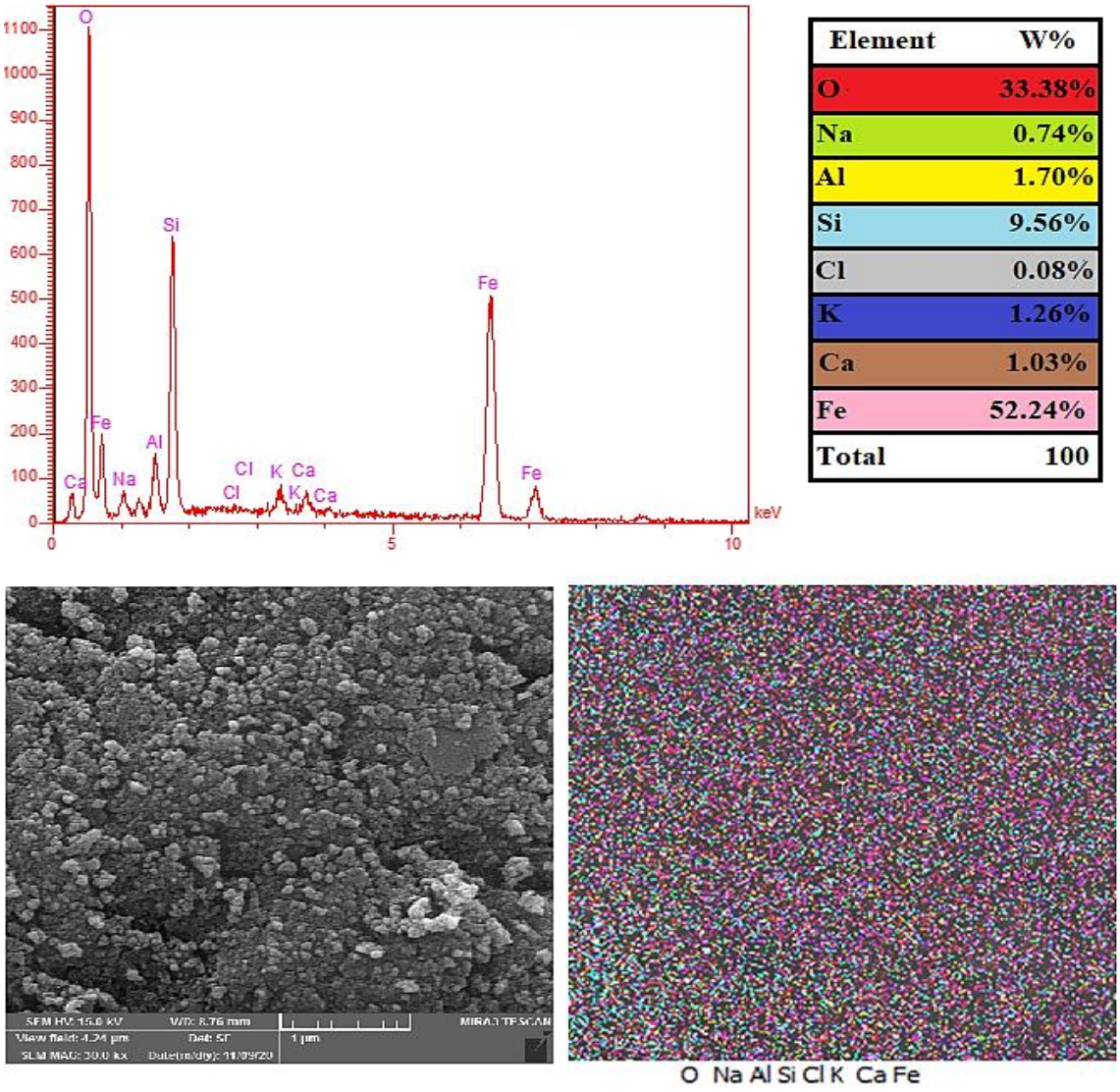

Element	W%
O	33.38%
Na	0.74%
Al	1.70%
Si	9.56%
Cl	0.08%
K	1.26%
Ca	1.03%
Fe	52.24%
Total	100

Fig. 5: SEM-EDX and mapping analysis results for Clin/Fe$_3$O$_4$

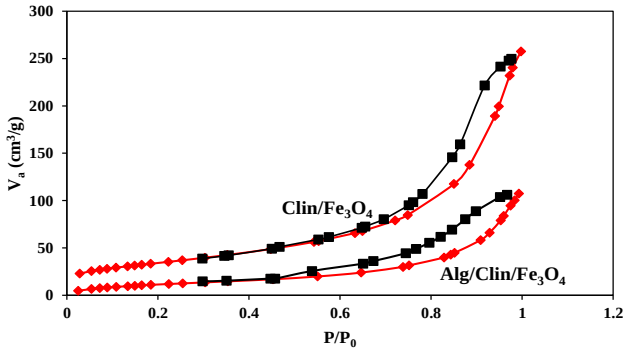

Fig. 6: Nitrogen adsorption-desorption isotherm for Clin/Fe$_3$O$_4$ and Alg/Clin/Fe$_3$O$_4$

may be explicable due to the existence of non-magnetic materials within the granule's structure - e.g., alginate. A simple magnet is able to segregate the synthesized Clin/Fe_3O_4 and Alg/Clin/Fe_3O_4 effortlessly, which is confirmed by all the VSM results.

The results of the BET analysis are displayed in Fig. 6. The values of specific surface area for Clin/Fe_3O_4 and Alg/Clin/Fe_3O_4 were ascertained as 123.17 m^2 /g and 44.88 m^2/g, in turn. The low values of the surface area of Alg/Clin/Fe_3O_4 can be due to the blockage of channels and pores of Clin/Fe_3O_4 by alginate during the granulation process, engendering a decrease in the total cross-sectional area of the ultimately obtained granules. Besides, the pore diameter of Clin/Fe_3O_4 and Alg/Clin/Fe_3O_4 adsorbents were measured as an average of 12.59 nm and 14.508 nm, respectively. According to the IUPAC classification, both

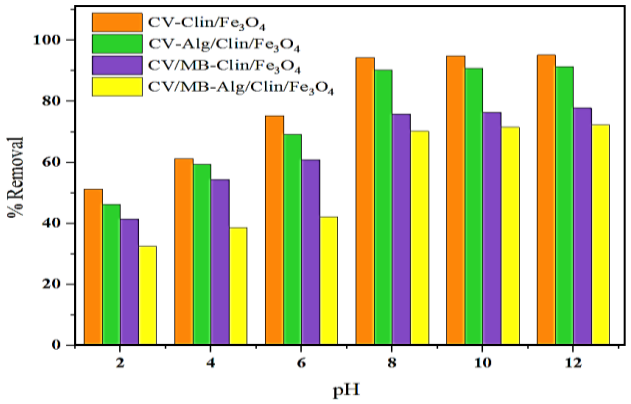

Fig. 7: Effect of pH on CV dye removal in single and CV/MB binary mixture solutions using Clin/Fe3O4 and Alg/Clin/Fe3O4

$Clin/Fe_3O_4$ and $Alg/Clin/Fe_3O_4$ have a mesoporous structure and the observed isotherm can be classified as a type IV isotherm with the H1 residue loop [40].

Adsorption study

Effect of pH

A solution's pH is considered one of the indispensable factors that can significantly affect adsorption capacity; because either the surface charge of an adsorbent or the ionization process of chemically activated sites are greatly influenced by pH [41]. Having considered this fact, pH's effect on the adsorption behavior of CV was studied both individually and in the presence of MB dye. Experiments were carried out using 1 g/L of the $Clin/Fe_3O_4$ and $Alg/Clin/Fe_3O_4$ adsorbents at the initial dye concentration of 10 mg/L at 25 °C for 60 min. The pH of all solutions was calibrated to values between 2 and 12 and the results are shown in Fig. 7. As observed, the percentage of CV dye removal in both single and CV/MB binary systems using $Clin/Fe_3O_4$ is higher than that using $Alg/Clin/Fe_3O_4$ at the same pH values. In point of fact, $Clin/Fe_3O_4$ adsorbent in the form of powder demonstrates more tendency towards CV removal compared to its granule form, for $Alg/Clin/Fe_3O_4$ provides less surface area collated with $Clin/Fe_3O_4$ [42]. As can be observed in Fig. 8, there is an increase in the adsorption of CV dye with an increase in pH value. Higher removal percentage in the alkaline conditions may be ascribed to the viable negative charge on the zeolite's surface. This phenomenon can be explained by the expedited association between positively charged dyes and the surface of the adsorbent accompanied by subsequent feasible electrostatic interactions among

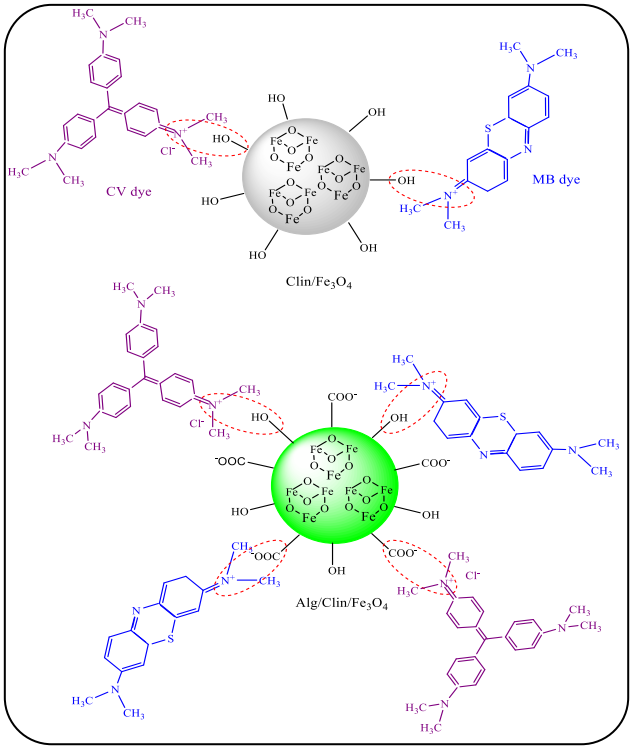

Fig. 8: Possible mechanism for interaction of CV and MB dye with Clin/Fe3O4 and Alg/Clin/Fe3O4

cationic dyes and molecules of adsorbent. However, the adsorption process may be intervened when it is carried on in a media with an acidic pH. Justification can be made by the presence of a higher concentration of H^+ ions on the adsorbent's surface which would lead to competing for H^+ ions with the dye cations for the adsorption sites [31, 43, 44]. The utmost efficiency of CV dye adsorption, within the investigated range of pH, employing both $Clin/Fe_3O_4$ and $Alg/Clin/Fe_3O_4$ was achieved at initial pH of 8. In the single system 94.32% and 90.21% and in the binary system 75.83% and 70.19% of CV dye was removed by $Clin/Fe_3O_4$ and $Alg/Clin/Fe_3O_4$, respectively. The initial pH of 8 was considered the optimal pH for further experiments. Although $Clin/Fe_3O_4$ and $Alg/Clin/Fe_3O_4$ have structural differences and the powder-shape adsorbent has a higher surface area, the dyes uptakes by $Alg/Clin/Fe_3O_4$ and $Clin/Fe_3O_4$ are optimal at the same pH. Regarding alkaline conditions, carboxyl (COO^-) groups within the structure of $Alg/Clin/Fe_3O_4$ lead to a surface with a more negative load, hence adsorption may enhance [42].

Adsorption efficiency soars relatively with increasing pH of the solution could be an indication that the CV dye adsorption mechanism could be explicated by chemical

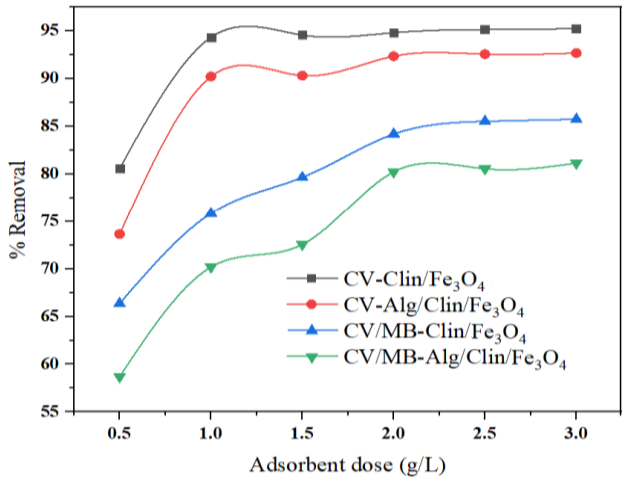

Fig. 9: Effect of adsorbent dose on CV dye removal in single and CV/MB binary mixture solutions using Clin/Fe$_3$O$_4$ and Alg/Clin/Fe$_3$O$_4$

interactions between the molecules of dyes and the adsorbents[31], a result that has been deduced previously from the FT-IR analysis. A viable foundation for dye adsorption can possibly be interaction forces between the N^+ groups related to CV molecules and OH groups affiliated with the surfaces of Clin/Fe_3O_4 and Alg/Clin/Fe_3O_4, acting as active sites. Correspondingly, N^+ groups of CV and MB molecules could attach to the carboxyl (COO^-) groups of alginate on the surface of the Alg/Clin/Fe_3O_4 [45]. The contemplated schematic related to the adsorption mechanism of CV dye on both Clin/Fe_3O_4 and Alg/Clin/Fe_3O_4 is illustrated in Fig 9.

Effect of the adsorbent dose

By altering the dose of Clin/Fe_3O_4 and Alg/Clin/Fe_3O_4 adsorbents between 0.5 to 3 g/L, the influence of this feature on the CV adsorption efficiency was investigated under the conditions of initial pH = 8 and temperature = 25°C. Moreover, the concentration of dye and contact time were adjusted to 10 mg/L and 60 min, respectively. The relationship between CV removal percentage and adsorbent dosage in both single (CV) and binary (CV/MB) systems is provided in Fig. 9. In accordance with the obtained results, initially the uptake of the investigated dye enhanced, subsequent to which it almost leveled off and remained steady by addition of more adsorbent and increasing the dosage of the adsorbent. Correspondingly, it can be observed that by increasing the dosage of Clin/Fe_3O_4 from 0.5 to 1 g/L, the removal of CV soared from 80.58% to 94.32%. Regarding the Alg/Clin/Fe_3O_4, it can be comprehended that increasing the granular adsorbent's dosage from 0.5 to 2 g/L remarkably enhanced the removal percentage of CV from 73.64% to 92.35%. Also, the data obtained on the CV dye removal in CV/MB mixture revealed that (66.37%, and 84.19%) and (58.71% and 80.23%) of CV was removed using (0.5 and 2 g/L) of Clin/Fe_3O_4 and Alg/Clin/Fe_3O_4 adsorbents, respectively. Moreover, the removal percentage's growth corresponding to a rise in the dosage of the adsorbent can be attributed to the enhanced number of adsorption sites on the surface of adsorbents. In other words, with the further increase of adsorbent dose, relatively more surface area of either Clin/Fe_3O_4 or Alg/Clin/Fe_3O_4 would be dispensed and available for the CV dye molecules [46, 47]. A further increase in the amount of adsorbent at higher adsorbent dosages, cannot cause a significant increase in the process efficiency. This indicates that the ratio of dyes molecules to the unoccupied sites is very low. Furthermore, the rivalry of the dye ions for the restricted and accessible binding sites, the nature of functional group on the adsorbent surface, ions contact overlapping or aggregation of adsorption sites and electrostatic interactions at higher adsorbent densities can reasonably justify low adsorption of dye at higher adsorbent dose [48]. It is worth mentioning that at the same dosage of adsorbent, the amount of dye adsorbed by the Clin/Fe_3O_4 was more the amount which was adsorbed by the Alg/Clin/Fe_3O_4. The obtained result can be associated to the fact that the specific area of powders is relatively higher than granules. Turning to the differences between the single and binary systems, binary system demonstrated lower removal due to the feasible competition between CV and MB for adsorption [49]. For further related experiments, the optimum dosages of Clin/Fe_3O_4 and Alg/Clin/Fe_3O_4 to reach the maximum CV dye adsorption was considered as 1g/L and 2 g/L, respectively in single system and as 2 g/L and 2 g/L, respectively in binary mixture system.

Effect of contact time

In order to find out the required time for attaining the equilibrium for CV adsorption onto Clin/Fe_3O_4 and Alg/Clin/Fe_3O_4 in single and CV/MB binary mixture solutions, the contact time ranged between 5 to 120 min. Other variables i.e., 10 mg/L for the initial concentration of dye, initial pH of 8, optimum dosages of adsorbents (mentioned in the previous section), and the temperature of 25°C were fixed constant. The obtained results are

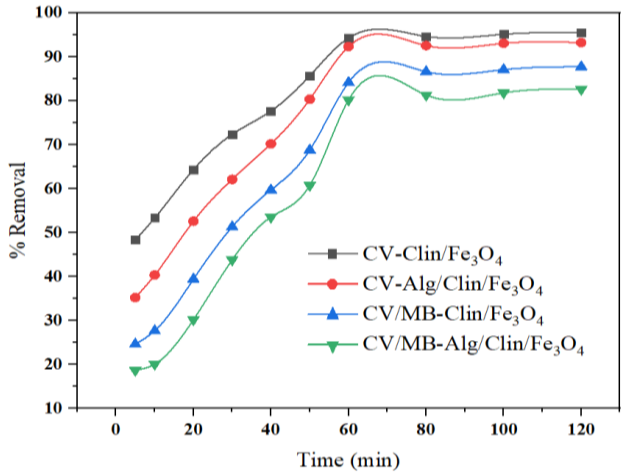

Fig. 10: Effect of contact time on CV dye removal in single and CV/MB binary mixture solutions using Clin/Fe3O4 and Alg/Clin/Fe3O4

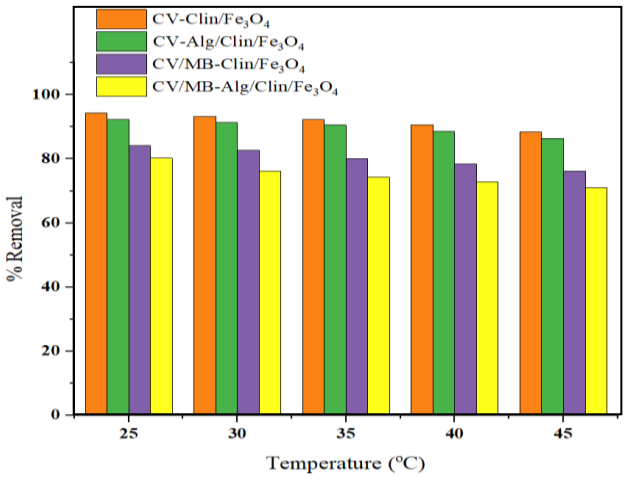

Fig. 11: Effect of temperature on CV dye removal in single and CV/MB binary mixture solutions using Clin/Fe3O4 and Alg/Clin/Fe3O4

represented in Fig. 10. As anticipated, during the initial stages of the process, the percentage of the removal went up promptly by enhancing the contact time. The major amount of the CV dye adsorption ensued within the beginning contact times; however, the adsorption rate decreased subsequent to 60 min and additional enhancement of contact time did not result in a further rise in the dye removal percentage on either Clin/Fe_3O_4 or Alg/Clin/Fe_3O_4. The increase in the CV adsorbed amount in the first steps might be justified by the adsorption on the external surfaces as a consequence of vacancy and availability of more adsorption sites on the adsorbent during the initial stages, which were positioned on the external surface. However, as time passed, it became slower and reached equilibrium owing to the developed accumulation in the internal surface of adsorbents in addition to the reduced number of reachable yet active sites on the adsorbent's surface, which cause a decline in the rate of dye adsorption [50]. At contact time >60min, there was no considerable change in dye removal. Therefore, the equilibrium time for the removal of CV dye individually and in the presence of MB using both adsorbents was determined as 60 min when the efficiencies were 94.32% and 92.35% in the single system and as 84.19% and 80.23% in the binary system reached by Clin/Fe_3O_4 and Alg/Clin/Fe_3O_4, respectively.

Effect of temperature

The temperature influence on CV dye removal in single and CV/MB binary systems using Clin/Fe_3O_4 and Alg/Clin/Fe_3O_4 was performed at various temperatures including 25, 30, 35, 40, and 45°C under conditions of pH 8, optimum dosages of adsorbents mentioned in section 3.2.2- and 60 min contact time. The obtained results are presented in Fig. 11. The results exhibited that the removal percentage of CV in a single system onto Clin/Fe_3O_4 and Alg/Clin/Fe_3O_4 was reduced from 94.32% to 88.36% and from 92.35% to 86.59%, respectively upon increasing the temperature from 25 to 45°C and, in the CV/MB binary system, it was decreased from 84.19% to 76.28% and from 80.23% to 70.96%, respectively. This indicates that the adsorption of the CV on both adsorbents is an exothermic process. The reduction in the adsorption of dyes at higher temperatures can be rationalized by the alteration or damage of the active adsorbent sites in the adsorbent structure and also the eroded and weakened supportive forces between the adsorbent's active sites and dye. Furthermore, the increasing temperature can advance the tendency of adsorbed dye molecules to separate from the surface of the adsorbent into the solution [51]. Therefore, 25°C was selected as the optimum solution temperature for the adsorption of CV dye employing either Clin/Fe_3O_4 or Alg/Clin/Fe_3O_4.

Effect of initial dyes concentration

The influence of CV and MB commencing concentration on its removal efficiency in single and binary systems using Clin/Fe_3O_4 and Alg/Clin/Fe_3O_4 was performed at varying dye concentrations ranging from 10-50 mg/L. The other adsorption parameters were kept constant throughout the experiments; under conditions of pH 8, optimum dosages

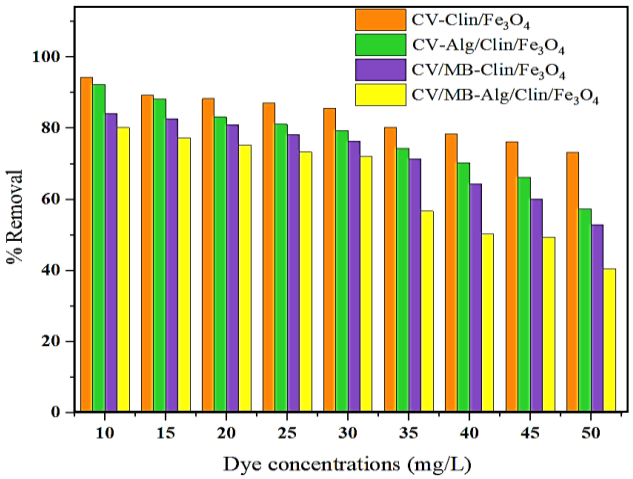

Fig. 12: Effect of initial dyes concentration on CV dye removal in single and CV/MB binary mixture solutions using Clin/Fe3O4 and Alg/Clin/Fe3O4

of adsorbents mentioned in section 3.2.2, 60 min contact time, and temperature of 25 °C. The obtained outcomes are shown in Fig. 12. According to the results, the efficiency of the CV adsorption process in the single system using Clin/Fe_3O_4 and Alg/Clin/Fe_3O_4 decreased from 95.78% and 98.34% to 36.38% and 55.34%, respectively. In the binary system, the removal percentage of CV onto Clin/Fe_3O_4 and Alg/Clin/Fe_3O_4 decreased from 84.19% to 76.28% and from 80.23% to 70.96%, respectively. A rise in the concentration of dye resulted in a decrease in the efficiency of the adsorption, which can be associated with the reduced availability of vacant adsorption sites due to their saturation at high dye concentrations and also to the increase of electrostatic repulsion force between the surface of the adsorbent and molecules of dye [52]. Thus, the maximum efficiency of CV adsorption in single and CV/MB mixture solutions using both adsorbents was obtained at 10 mg/L.

Adsorption isotherms

One of the important features of designing a system for adsorption is the adsorption isotherm, which describes how the adsorbent surface and the contaminants interact at an equilibrium state. The three most common isotherm models including Langmuir, Freundlich, and Dubinin–Radushkevich (D-R) opted to investigate the behavior, related to the equilibrium state, of the adsorption process for the CV dye employing both Clin/Fe_3O_4 and Alg/Clin/Fe_3O_4. Turning to the Langmuir isotherm, that is used by assuming that monolayer adsorption takes place

Table 2: Isotherm's constants and parameters obtained for CV dye removal in single and CV/MB binary mixture solutions by Clin/Fe3O4 and Alg/Clin/Fe3O4

		Adsorbent			
		Clin/Fe_3O_4		Alg/Clin/Fe_3O_4	
Isotherms	Parameters	CV	CV/MB	CV	CV/MB
Langmuir	q_m(mg/g)	44.052	15.797	16.528	11.467
	K_L(L/mg)	0.311	0.286	0.395	0.419
	R_L	0.849	0.688	0.767	0.546
	R^2	0.9843	0.9916	0.9929	0.9849
Freundlich	n	2.246	2.381	2.707	3.113
	K_F(mg/g)	12.062	4.253	5.435	4.123
	R^2	0.9827	0.8906	0.9614	0.7563
D-R	q_m(mg/g)	27.303	12.383	12.244	10.287
	$\beta\times10^{-7}$(mol^2/ kJ^2)	1.898	8.068	2.541	9.894
	E(kJ/mol)	1.623	0.787	1.402	0.71
	R^2	0.709	0.9255	0.7739	0.9261

At homogeneous active sites in the structure of the adsorbent. In the Freundlich model, it is assumed that adsorption occurs at a heterogeneous and rough surface. The D-R model is used to detect the chemical or physical adsorption mechanism based on the assumption that potential theory supposes heterogeneous surfaces. The linear equations of the isotherm models used in this study are as follows [53]:

Langmuir: $$\frac{C_e}{q_e} = \frac{1}{q_m K_L} + \frac{C_e}{q_m}, \quad R_L = \frac{1}{1+K_L C_O} \tag{3}$$

Freundlich: $$\ln q_e = \ln K_F + \frac{1}{n}\ln C_e \tag{4}$$

D-R: $$\varepsilon = RT\ln(1+\frac{1}{C_e}), \quad E = \frac{1}{\sqrt{2\beta}} \tag{5}$$

that, C_e (mg/L) represents equilibrium concentration, q_e (mg/g) and q_m (mg/g) stand for equilibrium adsorption capacity and the maximum adsorption capacity, respectively. K_L (L/mg) symbolizes Langmuir constant, R_L indicates the adsorption behavior and C_o is the initial dye concentration; k_F and n are Freundlich model constants, universal constant of gases is represented by R (8.314 J/mol.K), T (K) stands for absolute temperature, ε is Polanyi coefficient, E (kJ/mol) is the mean adsorption energy, and β is the adsorption energy constant (mol^2/J^2). Fig. 13 gives the linear fitting plots of the mentioned isotherms models and all the corresponding values of the constants along with correlation coefficients R^2 are also calculated and summarized in Table 2.

The adsorption data is well confirmed by Langmuir isotherm, regarding the correlation coefficients, which

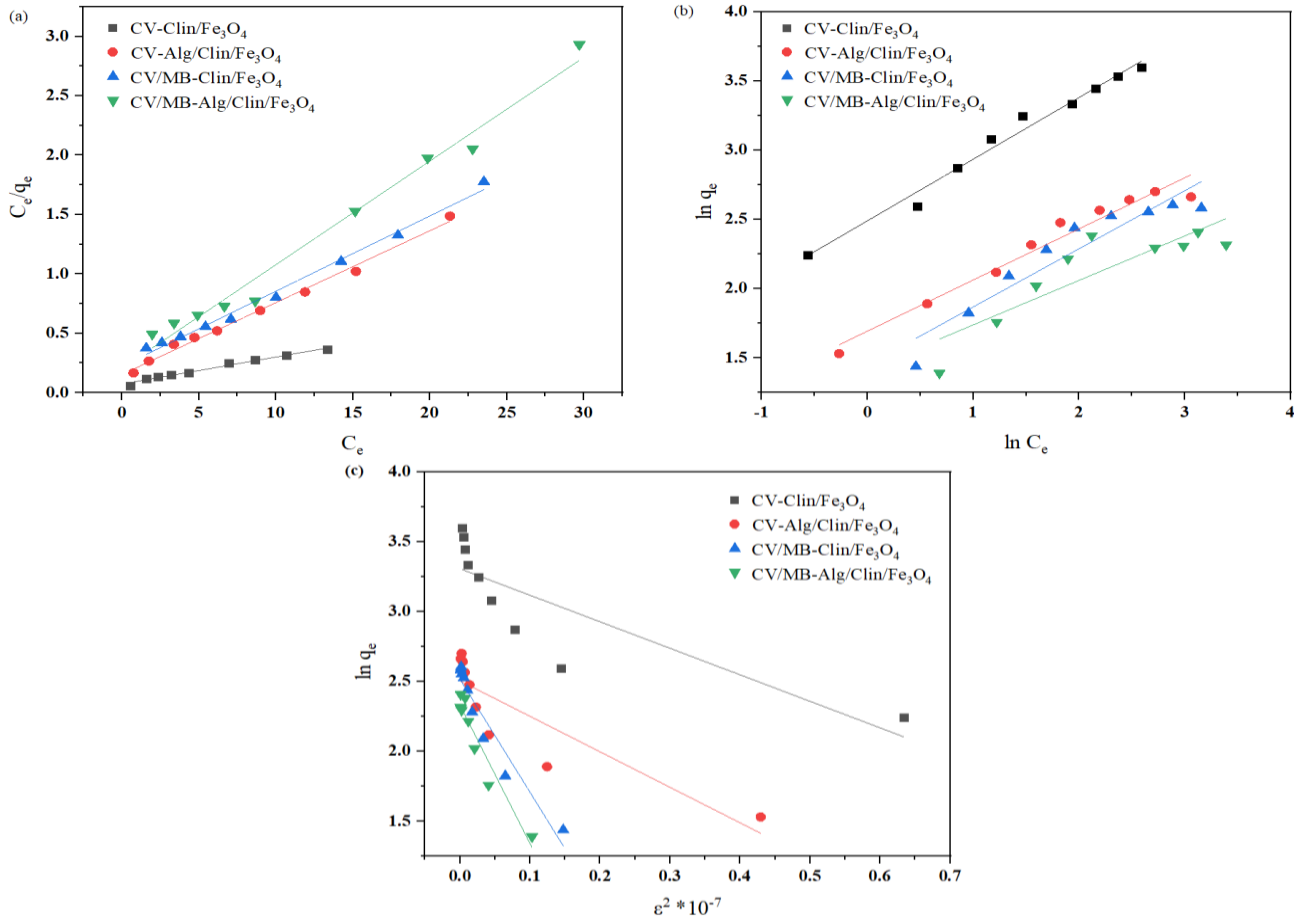

Fig. 13. (a) Langmuir, (b) Freundlich, and (c) D-R model isotherms for CV adsorption in single and binary systems by Clin/Fe3O4 and Alg/Clin/Fe3O4

means the Langmuir isotherm model can describe equilibrium adsorption features more preferable than Freundlich or D–R models. This finding emphasizes that surface of the adsorbents is homogeneous and monolayer as well as equivalent.

The maximum monolayer adsorption capacity (q_{max}) calculated for Clin/Fe_3O_4 and Alg/Clin /Fe_3O_4 regarding CV dye was 44.662 mg/g and 16.528 mg/g, in turn, in the single system; and it was computed to be 15.797 mg/g and 11.476 mg/g, respectively, in the CV/MB binary system. The value of R_L and n parameters calculated from the Langmuir and Freundlich models confirmed the adsorption is favorable and physical in nature, because the n>1 and R_L values are in the range of 0-1 [54]. The value of parameter E for Clin/Fe_3O_4 and Alg/Clin/Fe_3O_4 adsorbents in a single system was obtained as 1.623 kJ/mol and 1.402 kJ/mol, respectively. In the binary system, E was found to be 0.787 kJ/mol and 0.71 kJ/mol for Clin/Fe_3O_4 and Alg/Clin/Fe_3O_4, respectively. The E value obtained gives information on the adsorption mechanism; on the condition that the calculated value of E is less than 8 kJ/mol, the adsorption process is taken place in a physical type, but if the provided value ranged from 8 to 16 kJ/mol, the adsorption continues chemically. Since E< 8 kJ/mol, it indicates that the adsorption process of CV in single or binary systems towards both of the adsorbents proceeds physically. A comparison between the maximum adsorption capacity of Clin/Fe_3O_4 and Alg/Clin/Fe_3O_4 and also other adsorbents used in the literature towards CV dye removal were summarized in Table 3. As seen, the both Clin/Fe_3O_4 and Alg/Clin/Fe_3O_4 adsorbents possessed a greater adsorption capacity collated with the listed adsorbents for the CV dye removal in single system, either as powder or granule. It is noteworthy that the q_{max} of Alg/Clin/Fe_3O_4 granules utilized in current work has proved to be higher than some of the adsorbents in powder form used in the literature, hence it demonstrates its remarkable potential for removing CV dye. No data was found

Table 3: Comparison of maximum adsorption capacity q_{max} (mg/g) of various adsorbents towards CV dye in single and binary system.

Adsorbent	q_{max} (mg/g)		Reference
	single system	binary system	
	CV	CV/MB	
TLAC/Chitosan granules	13.698	-	[55]
Gracilaria corticata Seaweed Activated Carbon/Zn/Alginate granules	6.694	-	[56]
poly(acrylamide)-kaolin composite hydrogel	25	-	[57]
polyacrylonitrile/ -cyclodextrin/graphene oxide (powder)	15.48	-	[58]
Sugarcane Fiber (powder)	10.44	-	
Bottom ash	-	3.06	[59]
cotton fiber–graphene oxide	-	19.23	[60]
Clin/Fe_3O_4 nanocomposite (powder)	44.052	15.797	This work
Alg/Clin/Fe_3O_4 nanocomposite granules	16.528	11.467	This work

on using granular adsorbents for CV dye removal in CV/MB mixture solution in the literature, however both Clin/Fe_3O_4 and Alg/Clin/Fe_3O_4 still show an acceptable level of efficiency towards CV in binary system. All these results confirm that not only Fe_3O_4 nanoparticles are effectively placed in the structure of Clin/Fe_3O_4 powder but also using simple sodium alginate gelation method has been successfully applied to reform the powders into Alg/Clin/Fe_3O_4 granules with expanded porous structure. The introduced low-cost natural adsorbents in this work seem more practical to use, sustainable and fairly cheap prepared from a mineral material rather than other adsorbents that require more chemicals to produce.

Adsorption Kinetics

Study of adsorption kinetics is proved to be effective in both determining the adsorption mechanism and showing the interaction between adsorbent and dye ions in solution. The four well-known models which are Pseudo-First-Order (PFO), Pseudo-Second-Order (PSO), Intraparticle diffusion, and Elovich were opted for the description of CV dye adsorption on Clin/Fe_3O_4 and Alg/Clin/Fe_3O_4 in a single and binary system. Mathematical equations of PFO, PSO, Intraparticle diffusion, and Elovich kinetic models are given in Eqs. (6) to (9), respectively [61]:

$$\log(q_e - q_t) = \log q_e - \frac{k_1 t}{2.303} \quad (6)$$

$$\frac{t}{q_t} = \frac{1}{k_2 q_e^2} + \frac{t}{q_e} \quad (7)$$

$$q_t = k_i t^{1/2} + C \quad (8)$$

$$q_t = \frac{1}{\beta}\ln(\alpha\beta) + \frac{1}{\beta}\ln t \quad (9)$$

q_e (mg/g) represents equilibrium adsorption capacity, q_t (mg/g) stands for the amounts of dye adsorbed at time t (min), k_1 (min^{-1}) is the PFO kinetics constant, t indicates the time, k_2 (min^{-1}) is PSO kinetics constant, k_i is the intraparticle diffusion rate constant, C symbolizes a constant for the thickness of the boundary layer, α (mg/g.min) and β (g/mg) are the initial adsorption rate and the desorption constant, respectively. The linear plots for mentioned kinetic models are illustrated in Fig. 14 and their corresponding parameters and constants are provided in Table 4. The obtained results indicate that the PSO model has a better description of the adsorption of the CV in the single and binary systems onto Clin/Fe_3O_4 and Alg/Clin/Fe_3O_4 with a higher correlation coefficient (R^2) close to 1 in collation with previously investigated kinetic models. Moreover, the equilibrium capacity values (q_e) were computed using the PSO model for CV adsorption by Clin/Fe_3O_4 and Alg/Clin/Fe_3O_4 were obtained as 10.438 mg/g and 5.417 mg/g in the single system, and were derived as 5.583 mg/g and 5.543 mg/g in the binary system, in turn, which are closely match with the experimental adsorption values ($q_{e,exp}$). While the corresponding values of q_e calculated from the PFO kinetic model; (2.585 mg/g plus 2.385 mg/g in the single system and 2.284 mg/g plus 2.081 mg/g in the binary system reached by Clin/Fe_3O_4 and Alg/Clin/Fe_3O_4, respectively), show significant differences with q_e calculated from the experimental data. This data confirms that the PFO model is not well-suited regards the representation of the kinetic behavior for the process of CV adsorption. Based on the parameters obtained from the intraparticle diffusion model, the CV adsorption mechanism may be implied

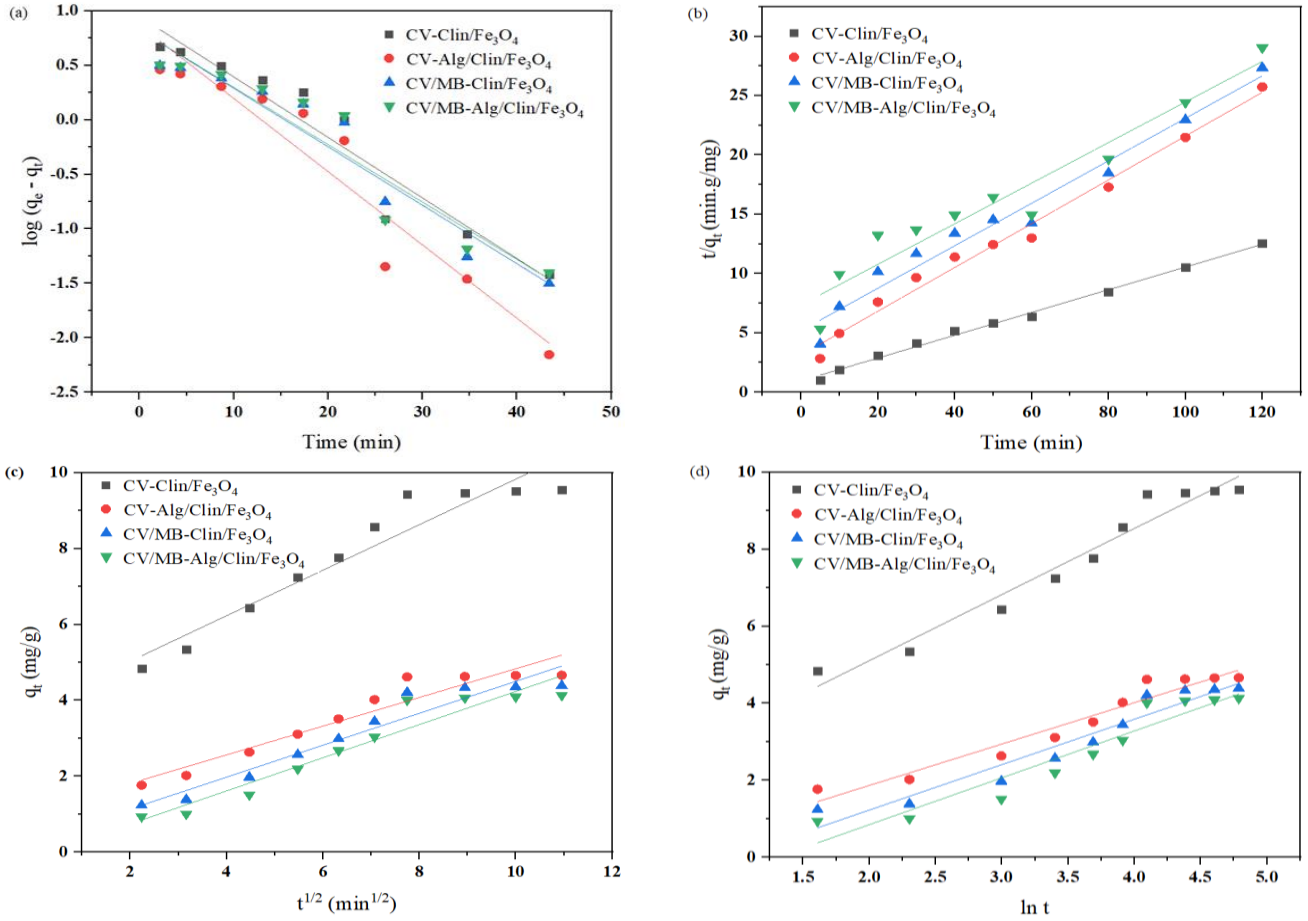

Fig. 14: Kinetic plots of (a) pseudo-first-order (b) pseudo-second-order (c) intraparticle diffusion and (d) Elovich model for CV dye adsorption in single and binary systems by Clin/Fe3O4 and Alg/Clin/Fe3O4

as three steps. Regarding the initial step, which happens more quickly, dye molecules reach the external surface of Clin/Fe_3O_4 and Alg/Clin/Fe_3O_4 adsorbents. In the second step, intraparticle diffusion is occurred and dye molecules are diffused to the internal cavities of the adsorbents. The third step which is corresponded to the adsorption process on the adsorption sites, takes place in a very slow rate due to the reduction of dyes concentrations in the medium [62]. With respect to the Elovich model for the CV dye adsorption process in a single and binary system for both adsorbents, the calculated values for α were higher β. In another words, adsorption rate seems to be rather higher than the desorption rate [63].

Thermodynamic parameters

The study of thermodynamic on the adsorption of CV dye from single (CV) and binary (CV/MB) systems on Clin/Fe_3O_4 and Alg/Clin/Fe_3O_4 adsorbents were evaluated to determine the parameters of entropy (ΔS°), enthalpy (ΔH°), and Gibbs free energy (ΔG°). The mentioned parameters were computed by the following equations [64]:

$$k_d = \frac{q_e}{C_e} \quad (10)$$

$$\ln k_d = \frac{\Delta S^\circ}{R} - \frac{\Delta H^\circ}{RT} \quad (11)$$

$$\Delta G^\circ = -RT \ln k_d \quad (12)$$

that k_d represents the equilibrium constant, q_e (mg/g) stands for equilibrium adsorption capacity and C_e (mg/L) represents the equilibrium constant. R (8.314 J/mol.K) and T (K) symbolize the universal gas constant and the absolute temperature, respectively. Considering Fig. 15, from the incline of the intercept of ln k_d vs. 1/T curve, both ΔH° and ΔS° values are computed. Table 5 provides the summary of the calculated values for the thermodynamic parameters. The negative values of ΔG° for the adsorption of CV dye in all cases indicate that the adsorption is thermodynamically favorable and spontaneous and hence CV molecules have a high affinity to be adsorbed

Table 4: Kinetic parameters for CV dye adsorption in single and binary system using Clin/Fe$_3$O$_4$ and Alg/Clin/Fe$_3$O$_4$

Models	Parameters	Adsorbent			
		Clin/Fe_3O_4		Alg/Clin/Fe_3O_4	
		CV	CV/MB	CV	CV/MB
Pseudo first-order	q_e(mg/g)	2.585	2.284	2.385	2.282
	$q_{e,exp}$(mg/g)	9.555	4.387	4.662	4.132
	k_1(min^{-1})	0.128	0.123	0.154	0.121
	R^2	0.9296	0.9332	0.9151	0.9061
Pseudo second-order	q_e(mg/g)	10.438	5.583	5.417	5.844
	$q_{e,exp}$(mg/g)	9.555	4.387	4.662	4.132
	k_2 (min^{-1})	0.009	0.006	0.01	0.003
	R^2	0.9951	0.9708	0.9873	0.9342
Elovich model	α(mg/g.min)	4.545	0.847	0.824	0.33
	β(g/mg)	0.582	0.45	0.93	0.8221
	R^2	0.9561	0.9316	0.9428	0.9112
Intraparticle diffusion	k_i(mg/g.$min^{1/2}$)	0.599	0.421	0.378	0.436
	C	3.833	0.291	1.049	0.133
	R^2	0.919	0.9344	0.9195	0.926

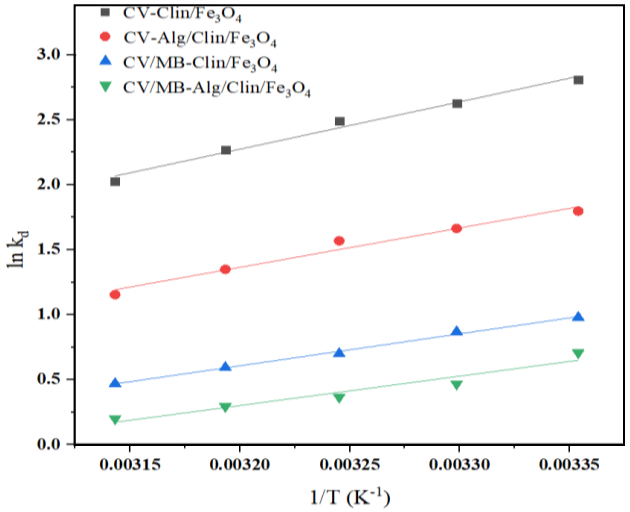

Fig. 15: The linear relation of ln k_d vs. 1/T to determine thermodynamic parameters

by Clin/Fe_3O_4 and Alg/Clin/Fe_3O_4. Furthermore, the ΔG° values were determined in the range of 0-20 kJ/mol suggesting the predominance of physical mechanisms in the adsorption. Also, the decrease of ΔG° by rising the temperature indicated that the adsorption of CV dye was more favorable at lower temperatures [65]. The values of ΔH° for CV dye adsorption using Clin/Fe_3O_4 and Alg/Clin/Fe_3O_4 from CV single solution were obtained as -30.287 kJ/mol and -25.186 kJ/mol and from CV/MB binary solution were found to be -20.425 kJ/mol and -18.816 kJ/mol, in turn. In addition, the negative values of ΔH° revealed that the adsorption of CV dye for all cases studied was exothermic. In addition, regarding the values of ΔH°<40 kJ/mol, it can be concluded that the physisorption with mainly acting of van der Waals' forces is predominant during the process of adsorption. However, it should be mentioned that the obtained kinetic result conformed to a PSO model which is an indication for the effectiveness of the chemical mechanism during the process of adsorption. Hence, this could be disputed that the adsorption of CV dye on either Clin/Fe_3O_4 or Alg/Clin/Fe_3O_4 adsorbents is a relatively complex process. Finally, a negative value of the ΔS° parameter indicated that a decrease in the accidental collisions of the adsorbents surface and contaminant ions is taken place during the adsorption of CV [66].

Table 5: Thermodynamic constants and parameters for CV dye adsorption in single and binary system using Clin/Fe$_3$O$_4$ and Alg/Clin/Fe$_3$O$_4$

Adsorbent	T (°C)	ΔG° (kJ/mol)	ΔH° (kJ/mol)	ΔS° (J/mol)
CV-Clin/Fe_3O_4	25	-6.964	-30.287	-78.005
	30	-6.625		
	35	-6.385		
	40	-5.91		
	45	-5.361		
CV/MB-Clin/Fe_3O_4	25	-2.427	-20.425	-60.3114
	30	-2.189		
	35	-1.795		
	40	-1.545		
	45	-1.241		
CV-Alg/Clin/Fe_3O_4	25	-4.456	-25.186	-69.2481
	30	-4.193		
	35	-4.019		
	40	-3.51		
	45	-3.054		
CV/MB-Alg/Clin/Fe_3O_4	25	-1.753	-18.816	-57.7091
	30	-1.177		
	35	-0.938		
	40	-0.765		
	45	-0.529		

Desorption studies

The reusability and desorption properties are some of the significant factors that need to be checked for the acceptance of an adsorbent in an industrial scale. For an efficient and effective adsorbent, both high adsorption

Table 6: CV desorption percentage from loaded Clin/Fe_3O_4 and Alg/Clin/Fe_3O_4 at different reagents

Desorbing reagent	%Desorption	
	Clin/Fe_3O_4	Alg/Clin/Fe_3O_4
ethanol	41.51	31.44
methanol	14.76	10.39
0.1 M HCl	5.31	5.37
0.5M NaCl	6.28	4.28
0.5M $CaCl_2$	6.99	5.81
ethanol + 0.5 M $CaCl_2$	65.47	60.19

capacity and good regeneration performance are expected to be economically viable [67]. The CV dye desorption studies were carried out using different desorption reagents including methanol, ethanol, 0.5M NaCl, 0.1M HCl, 0.5M $CaCl_2$, and ethanol + 0.5M $CaCl_2$. The percentage of desorption for CV-loaded Clin/Fe_3O_4 and Alg/Clin/Fe_3O_4 at different reagents is shown in Table 6. Choosing the desorbing reagent HCl was based on the observations showed superior adsorption efficiency at alkaline pHs (see Fig. 7), hence suggesting an acidic solution of 0.1 M HCl in order to recycle the adsorbents at the first level. However, by using HCl desorption reagent the granules started to deteriorate just after the first cycle. By using 0.5M NaCl and 0.5M $CaCl_2$ solutions as desorption reagents, the low desorption percentages of 6.28% and 6.99%, respectively for Clin/Fe_3O_4 and 4.28% and 5.81%, respectively for Alg/Clin/Fe_3O_4 were achieved. This result showed that solutions of salts cannot be a preferable alternative considering the desorption of cationic dyes. In the case of using organic compounds such as methanol and ethanol as regeneration reagents, a superior desorption efficiency was observed which might be due to the more solubility of dyes in organic solvents [68]. As an idea, ethanol + 0.5M $CaCl_2$ was contacted with both of the adsorbents loaded with CV dye, led to the highest level of desorption efficiencies as 65.47% and 60.19% for Clin/Fe_3O_4 and Alg/Clin/Fe_3O_4, respectively. As it can be observed, the Clin/Fe_3O_4 adsorbent desorption percentage is quite greater than the obtained percentage for Alg/Clin/Fe_3O_4 adsorbent, which might be attributed to the higher surface area of powder adsorbents rather than the granular ones. Considering all of the reagents opted for desorption, ethanol + 0.5M $CaCl_2$ proved to be the most efficient regarding the regeneration of Clin/Fe_3O_4 and Alg/Clin/Fe_3O_4 adsorbents, hence it was selected to perform the regeneration experiments for further cycles.

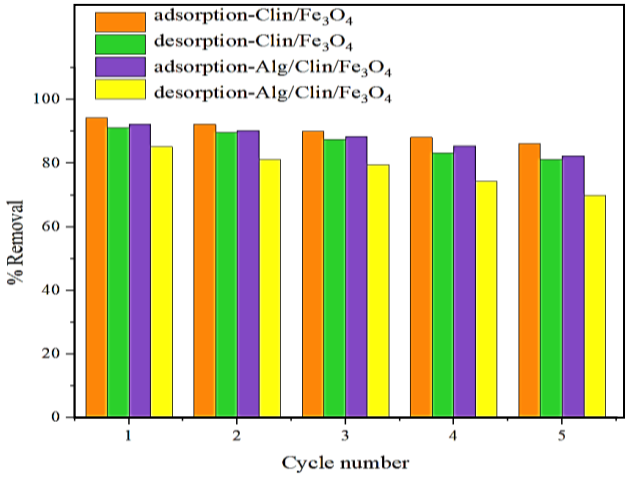

Fig. 16: Reusability of (a) Clin/Fe_3O_4, (b) Alg/Clin/Fe_3O_4 after five consecutive adsorption-desorption cycles

This may be found noteworthy that the existence of $CaCl_2$ in selected reagent solution can strengthen the granules by improved crosslinking and correspondingly would aid stabilizing the granules in case of several uses [69]. The experiments related to regeneration were carried out on Clin/Fe_3O_4 and Alg/Clin/Fe_3O_4 using ethanol + 0.5M $CaCl_2$ for five adsorption/desorption cycles and the outcomes are provided in Fig. 16. After five cycles of adsorption-desorption, the adsorption capacity of Clin/Fe_3O_4 and Alg/Clin/Fe_3O_4 reduced from 94.32 to 86.24% and 85.2 to 69.87%, respectively. This decrease in CV uptake might be explained by the probable changing of the adsorbent structure through the desorption phase, during which the adsorption sites could be blocked or lost [70]. All the obtained data from the adsorption-desorption tests illustrated that Clin/Fe_3O_4 and Alg/Clin/Fe_3O_4 can be considered as cost-effective, and environmentally friendly with good regenerative capacity for the sequestration of CV dye from aqueous solutions.

Electrical conductivity (EC) measurement

In the final part of the work, the electrical conductivity of MB, CV, and CV/MB solutions with the concentration of 10 mg/L and also real wastewater sampled from a dyeing unit was measured before and after being treated by Clin/Fe_3O_4 and Alg/Clin/Fe_3O_4 under optimal conditions (except for pH which was not adjusted). The results of this section are presented in Table 7. As seen, the EC of MB, CV, and CV/MB solutions after the adsorption process using Clin/Fe_3O_4 was reduced from 96.1 to 57.4 (μS/cm), 70.5 to 45.5 (μS/cm), and 76.4 to 55.3 (μS/cm) and after

Table 7: Measurement of electrical conductivity of MB, CV, CV/MB solutions and real wastewaters before and after adsorption process by Clin/Fe_3O_4 and Alg/Clin/Fe_3O_4

Sample	EC (μS/cm)	TDS (mg/L)	Decrease in EC (%)
MB- before adsorption	96.1	67.27	-
MB- after adsorption by Clin/Fe_3O_4	57.4	40.18	40.27
MB- after adsorption by Alg/Clin/Fe_3O_4	40.9	28.63	57.44
CV- before adsorption	70.5	49.35	-
CV- after adsorption by Clin/Fe_3O_4	45.5	31.85	35.46
CV- after adsorption by Alg/Clin/Fe_3O_4	31.2	21.84	55.74
MB/CV- before adsorption	76.4	35.48	-
MB/CV- after adsorption by Clin/Fe_3O_4	55.3	38.71	27.61
MB/CV- after adsorption by Alg/Clin/Fe_3O_4	43.7	30.59	42.80
Real textile wastewater- before adsorption	12340	11106	-
Real textile wastewater- after adsorption by Clin/Fe_3O_4	12280	11052	0.48
Real textile wastewater- after adsorption by Alg/Clin/Fe_3O_4	12260	11034	0.64

adsorption process using Alg/Clin/Fe_3O_4 was decreased from 96.1 to 40.9 (μS/cm), 70.5 to 31.2 (μS/cm), and 76.4 to 43.7 (μS/cm), respectively. The EC of real wastewater before treatment was 12340 (μS/cm) which is very high than the permissible limits (1000 μS/cm) (EPA standard) [28], indicating a very high degree of pollution. The EC of real wastewater after treatment using Clin/Fe_3O_4 and Alg/Clin/Fe_3O_4 was reduced to 12280 (μS/cm) and 12260 (μS/cm), respectively. This very low rate of reduction of electrical conductivity in the case of real wastewater compared to the prepared laboratory samples might be due to the presence of a wide range of different dyes and other substances such as dispersants, salts, acids, bases, and maybe heavy metals in dyeing effluents and also the complexity of the nature of these effluents affecting the adsorption. Despite the higher adsorption efficiency of Clin/Fe_3O_4 rather than Alg/Clin/Fe_3O_4, it should be noted that the EC decrease percentages using granular adsorbent, in all samples, were more noticeable. This observation might be attributed to the higher amounts of iron leakage in the case of Clin/Fe_3O_4 powder than Alg/Clin/Fe_3O_4 granule. To investigate the possible leakage of Fe_3O_4 to the solutions, both powder and granular-shaped adsorbents were embedded into deionized water at neutral, alkaline, and acidic pHs and stirred for 60 minutes. Then, AAS analysis was carried out to determine the iron concentration in the resulting solutions. The amount of iron in Clin/Fe_3O_4 and Alg/Clin/ Fe_3O_4 containing solutions was found as 0.18 mg/L and 0.06 mg/L at neutral pH, 0.25 mg/L and 0.12 mg/L at acidic pH, and 0.14 mg/L and 0.04 mg /L at alkaline pH, in turn. Considering the granular adsorbent, the leakage of Fe_3O_4 was significantly lower than that of powder-shaped adsorbent which can be due to encapsulation of the Clin/Fe_3O_4 adsorbent in a polymeric matrix. It is also worth mentioning that the published value by WHO standards as the tolerable limit of iron in drinking water is 0.3 mg/L [71]; however, in the case of industrial utilization, it is less than 0.2 mg/L [72]. Regarding the amount of Fe_3O_4 leakage, specifically adsorbents in the form of granules which are the most preferable, it appears to be significantly less than the tolerable limitation, hence it may not cause any detrimental or consequential environmental or health problems.

CONCLUSIONS

In the current investigation, Clin/Fe_3O_4 and Alg/Clin/Fe_3O_4 were synthesized and used to remove the CV dye from single and binary systems. The analysis of XRD, FT-IR, SEM, EDX, dot mapping, and BET was applied to identify the Clin/Fe_3O_4 and Alg/Clin/Fe_3O_4 structure and adsorption mechanisms. Influential parameters such as pH, temperature, contact time, adsorbent dosage, and initial concentration of dyes on the adsorption behavior were systematically investigated. The optimum value of pH=8 and adsorbent dose (1 or 2g/L depending on the adsorbent type), contact time 60 min, the temperature of 25°C, and dye concentrations of 10 mg/L were determined. The equilibrium data followed the Langmuir model (R^2 > 0.9). The maximum adsorption capacity (q_{max}) using Clin/Fe_3O_4 and Alg/Clin/Fe_3O_4 was ascertained

as 44.662 mg/g and 16.528 mg/g, in turn, in the single system and it was computed to be 15.797 mg/g and 11.476 mg/g, respectively in the binary system. Pseudo-first order kinetic was also fitted regarding the CV dye's adsorption in single and binary systems towards Clin/Fe_3O_4 and Alg/Clin/Fe_3O_4. The adsorption process was exothermic and thermodynamically spontaneous. According to the thermodynamic and kinetic results, it can be speculated that the adsorption of CV is considered a proportionately convoluted process, within which both physical adsorption and chemical adsorption coincide. Moreover, pointing to the excellent regeneration capacity, both Clin/Fe_3O_4 and Alg/Clin/Fe_3O_4 adsorbents are considered to be interesting materials for the uptake of toxic dyes from wastewater.

HIGHLIGHTS

- Novel magnetic adsorbents of Clin/Fe_3O_4 and Alg/Clin/Fe_3O_4 were synthesized.
- Clin/Fe_3O_4 and Alg/Clin/Fe_3O_4 were used to remove crystal violet dye in single and binary systems.
- The maximum capacity of crystal violet adsorption in single system was determined as 16 mg/g.
- The maximum capacity of crystal violet adsorption in binary system was determined as 11 mg/g
- Adsorption data were obeyed the PSO kinetic model.
- The electrical conductivity was reduced after treatment using Clin/Fe_3O_4 and Alg/Clin/Fe_3O

Received: Dec. 31, 2022; Accepted: May. 22, 2023

REFERENCES

[1] Mohanty S., Moulick S., Maji S.K., Adsorption/Photodegradation of Crystal Violet (Basic Dye) from Aqueous Solution by Hydrothermally Synthesized Titanate Nanotube (TNT), *J. Wat. Proc. Eng.*, **37:** 101428 (2020).

[2] Iran Manesh M., Sohrabi M.R., Mortazavi Nik S., Nanoscale Zero-Valent Iron Supported on Graphene Novel Adsorbent for the Removal of Diazo Direct Red 81 from Aqueous Solution: Isotherm, Kinetics, and Thermodynamic Studies, *Iran. J. Chem. Chem. Eng.(IJCCE),* **41(6):** 1844-1855 (2022).

[3] Oloo C.M., Onyari J.M., Wanyonyi W.C., Wabomba J.N., Muinde V.M., Adsorptive Removal of Hazardous Crystal Violet Dye Form Aqueous Solution Using Rhizophora Mucronata Stem-Barks: Equilibrium and Kinetics Studies, *Environmental Chemistry and Ecotoxicology*, **2:** 64-72 (2020).

[4] Ishaq M., Javed F., Amad I., Ullah H., Hadi F., Sultan S., Adsorption of Crystal Violet Dye from Aqueous Solutions onto Low-Cost Untreated and Naoh Treated Almond Shell, *Iran. J. Chem. Chem. Eng. (IJCCE),* **35(2):** 97-106 (2016).

[5] Pang X., Sellaoui L., Franco D., Netto M.S., Georgin J., Dotto G.L., Shayeb M.K.A., Belmabrouk H., Bonilla-Petriciolet A., Li Z., Preparation and Characterization of a Novel Mountain Soursop Seeds Powder Adsorbent and Its Application for the Removal of Crystal Violet and Methylene Blue from Aqueous Solutions, *Chem. Eng. J.*, **391:** 123617 (2020).

[6] Calimli M.H., Nas M.S., Burhan H., Mustafov S.D., Demirbas Ö., Sen F., Preparation, Characterization and Adsorption Kinetics of Methylene Blue Dye in Reduced-Graphene Oxide Supported Nanoadsorbents, *J. Mol. Liq.*, **309:** 113171 (2020).

[7] Eltaweil A.S., Elgarhy G.S., El-Subruiti G.M., Omer A.M., Carboxymethyl Cellulose/Carboxylated Graphene Oxide Composite Microbeads for Efficient Adsorption of Cationic Methylene Blue Dye, *International Journal of Biological Macromolecules*, **154:** 307-318 (2020).

[8] Motakef-Kazemi N., Asadi A., Methylene Blue Adsorption from Aqueous Solution Using Zn_2 (BDC) 2 (DABCO) Metal Organic Framework and Its Polyurethane Nanocomposite, *Iran. Jour. Chem. Chem. Eng.*, **41(12):** 4026-4038 (2022).

[9] Ganea I.-V., Nan A., Baciu C., Turcu R., Effective Removal of Crystal Violet Dye Using Neoteric Magnetic Nanostructures based on Functionalized Poly (Benzofuran-Co-Arylacetic Acid): Investigation of the Adsorption Behaviour and Reusability, *Nanomaterials*, **11(3):** 679 (2021).

[10] Wu Y.-H., Xue K., Ma Q.-L., Ma T., Ma Y.-L., Sun Y.-G., Ji W.-X., Removal of Hazardous Crystal Violet Dye by Low-Cost P-Type Zeolite/Carbon Composite Obtained from in Situ Conversion of Coal Gasification Fine Slag, *Microporous and Mesoporous Materials*, **312:** 110742 (2021).

[11] Jawad A.H., Abdulhameed A.S., Mastuli M.S., Acid-Factionalized Biomass Material for Methylene Blue Dye Removal: A Comprehensive Adsorption and Mechanism Study, *Journal of Taibah University for Science*, **14(1):** 305-313 (2020).

[12] Mohammadi R., Masoumi B., Mashayekhi R., Hosseinian A., Fe_3O_4/Polystyrene-Alginate Nanocomposite as a Novel Adsorbent for Highly Efficient Removal of Dyes, *Iranian Journal of Chemistry and Chemical Engineering (IJCCE)*, **41(11):** 3632-3645 (2022).

[13] Elsherif K., El-Dali A., Alkarewi A., Ewlad-Ahmed A., Treban A., Adsorption of Crystal Violet Dye onto Olive Leaves Powder: Equilibrium and Kinetic Studies, *Chemistry International*, **7(2):** 79-89 (2021).

[14] Sivalingam S., Sen S., Efficient Removal of Textile Dye Using Nanosized Fly Ash Derived Zeolite-X: Kinetics and Process Optimization Study, *Journal of the Taiwan Institute of Chemical Engineers*, **96:** 305-314 (2019).

[15] Alver E., Metin A.Ü., Anionic Dye Removal from Aqueous Solutions Using Modified Zeolite: Adsorption Kinetics and Isotherm Studies, *Chemical Engineering Journal*, **200:** 59-67 (2012).

[16] Qiu M., Qian C., Xu J., Wu J., Wang G., Studies on the Adsorption of Dyes into Clinoptilolite, *Desalination*, **243(1-3):** 286-292 (2009).

[17] Hernández-Montoya V., Pérez-Cruz M.A., Mendoza-Castillo D.I., Moreno-Virgen M., Bonilla-Petriciolet A., Competitive Adsorption of Dyes and Heavy Metals on Zeolitic Structures, *Journal of Environmental Management*, **116:** 213-221 (2013).

[18] Karadag D., Akgul E., Tok S., Erturk F., Kaya M.A., Turan M., Basic and Reactive Dye Removal Using Natural and Modified Zeolites, *Journal of Chemical & Engineering Data*, **52(6):** 2436-2441 (2007).

[19] Molla Mahmoudi M., Nadali A., Soheil Arezoomand H.R., Mahvi A.H., Adsorption of Cationic Dye Textile Wastewater Using Clinoptilolite: Isotherm and Kinetic Study, *The Journal of the Textile Institute*, **110(1):** 74-80 (2019).

[20] Badeenezhad A., Azhdarpoor A., Bahrami S., Yousefinejad S., Removal of Methylene Blue Dye from Aqueous Solutions by Natural Clinoptilolite and Clinoptilolite Modified by Iron Oxide Nanoparticles, *Molecular Simulation*, **45(7):** 564-571 (2019).

[21] Jeon C., Adsorption Behavior of Silver Ions from Industrial Wastewater onto Immobilized Crab Shell Beads, *Journal of Industrial and Engineering Chemistry*, **32:** 195-200 (2015).

[22] Majid Z., Abdul Razak A.A., Noori W.A.H., Modification of Zeolite by Magnetic Nanoparticles for Organic Dye Removal, *Arabian Journal for Science & Engineering (Springer Science & Business Media BV)*, **44(6):** (2019).

[23] Lee C., Jung J., Pawar R.R., Kim M., Lee S.-M., Arsenate and Phosphate Removal from Water Using Fe-Sericite Composite Beads in Batch and Fixed-Bed Systems, *Journal of Industrial and Engineering Chemistry*, **47:** 375-383 (2017).

[24] Hassani A., Soltani R.D.C., Karaca S., Khataee A., Preparation of Montmorillonite–Alginate Nanobiocomposite for Adsorption of a Textile Dye in Aqueous Phase: Isotherm, Kinetic and Experimental Design Approaches, *Journal of Industrial and Engineering Chemistry*, **21:** 1197-1207 (2015).

[25] Aichour A., Zaghouane-Boudiaf H., Iborra C.V., Polo M.S., Bioadsorbent Beads Prepared from Activated Biomass/Alginate for Enhanced Removal of Cationic Dye from Water Medium: Kinetics, Equilibrium and Thermodynamic Studies, *Journal of Molecular Liquids*, **256:** 533-540 (2018).

[26] Ali N.S., Mo K., Kim M., A Case Study on the Relationship between Conductivity and Dissolved Solids to Evaluate the Potential for Reuse of Reclaimed Industrial Wastewater, *KSCE Journal of Civil Engineering*, **16(5):** 708-713 (2012).

[27] Choo-In S., The Relationship between the Total Dissolved Solids and the Conductivity Value of Drinking Water, Surface Water, and Waste Water, *Indonesian Journal of Business, Technology and Sustainability (IJBTS)*, 11-16 (2019).

[28] Ali S., Nadeem R., Bhatti H.N., Hayat S., Ali S., Chatha S., Muneer M., Analyses and Treatment of Textile Effluents, *Int. J. Agric. Biol.*, **8:** 641-644 (2006).

[29] Foroutan R., Ahmadlouydarab M., Ramavandi B., Mohammadi R., Studying the Physicochemical Characteristics and Metals Adsorptive Behavior of CMC-G-HAp/Fe_3O_4 Nanobiocomposite, *Journal of Environmental Chemical Engineering*, **6(5):** 6049-6058 (2018).

[30] Tahmasebpoor M., Hosseini Nami S., Khatamian M., Sanaei L., Arsenate Removal from Contaminated Water Using Fe_2O_3-Clinoptilolite Powder and Granule, *Envir. Technol*, **43(1):** 116-130 (2020).

[31] Sahu S., Pahi S., Tripathy S., Singh S.K., Behera A., Sahu U.K., Patel R.K., Adsorption of Methylene Blue on Chemically Modified Lychee Seed Biochar: Dynamic, Equilibrium, and Thermodynamic Study, *Journal of Molecular Liquids*, **315:** 113743 (2020).

[32] Rashid J., Tehreem F., Rehman A., Kumar R., Synthesis Using Natural Functionalization of Activated Carbon from Pumpkin Peels for Decolourization of Aqueous Methylene Blue, *Science of the Total Environment*, **671:** 369-376 (2019).

[33] Kragović M., Pašalić S., Marković M., Petrović M., Nedeljković B., Momčilović M., Stojmenović M., Natural and Modified Zeolite—Alginate Composites. Application for Removal of Heavy Metal Cations from Contaminated Water Solutions, *Minerals*, **8(1):** 11 (2018).

[34] Afshin S., Rashtbari Y., Vosoughi M., Rehman R., Ramavandi B., Behzad A., Mitu L., Removal of Basic Blue-41 Dye from Water by Stabilized Magnetic Iron Nanoparticles on Clinoptilolite Zeolite, *Revista de Chimie*, **71(2):** 218-229 (2020).

[35] Antarnusa G., Suharyadi E., A Synthesis of Polyethylene Glycol (Peg)-Coated Magnetite Fe_3O_4 Nanoparticles and Their Characteristics for Enhancement of Biosensor, *Materials Research Express*, **7(5):** 056103 (2020).

[36] Kazemi J., Javanbakht V., Alginate Beads Impregnated with Magnetic Chitosan@ Zeolite Nanocomposite for Cationic Methylene Blue Dye Removal from Aqueous Solution, *Inter. J. Bio. Macr.*, **154:** 1426-1437 (2020).

[37] Hu X., Wang Y., Zhang L., Xu M., Formation of Self-Assembled Polyelectrolyte Complex Hydrogel Derived from Salecan and Chitosan for Sustained Release of Vitamin C, *Carbo. Poly.*, **234:** 115920 (2020).

[38] Gopanna A., Mandapati R.N., Thomas S.P., Rajan K., Chavali M., Fourier Transform Infrared Spectroscopy (FT-IR), Raman Spectroscopy and Wide-Angle X-Ray Scattering (WAXS) of Polypropylene (PP)/Cyclic Olefin Copolymer (COC) Blends for Qualitative and Quantitative Analysis, *Polymer Bulletin*, **76(8):** 4259-4274 (2019).

[39] Shen Y., Zhou P., Zhao S., Li A., Chen Y., Bai J., Han C., Wei D., Ao Y., Synthesis of High-Efficient Tio2/Clinoptilolite Photocatalyst for Complete Degradation of Xanthate, *Minerals Engineering*, **159:** 106640 (2020).

[40] Castro M.A.M., Oliveira T.P., Correia G.S., Oliveira M.M., Rangel J.H.G., Rodrigues S.F., Mercury J.M.R., Synthesis of Hydroxyapatite by Hydrothermal and Microwave Irradiation Methods from Biogenic Calcium Source Varying Ph and Synthesis Time, *Boletín de la Sociedad Española de Cerámica y Vidrio*, **61(1):** 35-41 (2020).

[41] Sukla Baidya K., Kumar U., Adsorption of Brilliant Green Dye from Aqueous Solution onto Chemically Modified Areca Nut Husk, *South African Journal of Chemical Engineering*, **35:** 33-43 (2021).

[42] Nordin A.H., Ahmad K., Xin L.K., Syieluing W., Ngadi N., Efficient Adsorptive Removal of Methylene Blue from Synthetic Dye Wastewater by Green Alginate Modified with Pandan, *Materials Today: Proceedings*, **39:** 979-982 (2021).

[43] Brião G.V., Jahn S.L., Foletto E.L., Dotto G.L., Highly Efficient and Reusable Mesoporous Zeolite Synthetized from a Biopolymer for Cationic Dyes Adsorption, *Coll. Surf. A: Physicochemical and Engineering Aspects*, **556:** 43-50 (2018).

[44] Wang W., Zhao Y., Bai H., Zhang T., Ibarra-Galvan V., Song S., Methylene Blue Removal from Water Using the Hydrogel Beads of Poly (Vinyl Alcohol)-Sodium Alginate-Chitosan-Montmorillonite, *Carbohydrate Polymers*, **198:** 518-528 (2018).

[45] Bayat M., Javanbakht V., Esmaili J., Synthesis of Zeolite/Nickel Ferrite/Sodium Alginate Bionanocomposite *via* a Co-Precipitation Technique for Efficient Removal of Water-Soluble Methylene Blue Dye, *Inter. J. Bio. Macro.*, **116:** 607-619 (2018).

[46] Mouni L., Belkhiri L., Bollinger J.-C., Bouzaza A., Assadi A., Tirri A., Dahmoune F., Madani K., Remini H., Removal of Methylene Blue from Aqueous Solutions by Adsorption on Kaolin: Kinetic and Equilibrium Studies, *Applied Clay Science*, **153:** 38-45 (2018).

[47] Zhu Y., Yi B., Yuan Q., Wu Y., Wang M., Yan S., Removal of Methylene Blue from Aqueous Solution by Cattle Manure-Derived Low Temperature Biochar, *RSC advances*, **8(36):** 19917-19929 (2018).

[48] Tahir N., Bhatti H.N., Iqbal M., Noreen S., Biopolymers Composites with Peanut Hull Waste Biomass and Application for Crystal Violet Adsorption, *International Journal of Biological Macromolecules*, **94:** 210-220 (2017).

[49] Pan Y., Shi X., Cai P., Guo T., Tong Z., Xiao H., Dye Removal from Single and Binary Systems Using Gel-Like Bioadsorbent based on Functional-Modified Cellulose, *Cellulose*, **25(4):** 2559-2575 (2018).

[50] El Khomri M., El Messaoudi N., Dbik A., Bentahar S., Lacherai A., Chegini Z.G., Iqbal M., Organic Dyes Adsorption on the Almond Shell (Prunus Dulcis) as Agricultural Solid Waste from Aqueous Solution in Single and Binary Mixture Systems, *Biointerface Research in Applied Chemistry*, **12(2):** 2022-2040 (2021).

[51] Tahir M.A., Bhatti H.N., Iqbal M., Solar Red and Brittle Blue Direct Dyes Adsorption onto Eucalyptus Angophoroides Bark: Equilibrium, Kinetics and Thermodynamic Studies, *Journal of Environmental Chemical Engineering*, **4(2):** 2431-2439 (2016).

[52] Ma T., Wu Y., Liu N., Wu Y., Hydrolyzed Polyacrylamide Modified Diatomite Waste as a Novel Adsorbent for Organic Dye Removal: Adsorption Performance and Mechanism Studies, *Polyhedron*, **175:** 114227 (2020).

[53] Feng M., Yu S., Wu P., Wang Z., Liu S., Fu J., Rapid, High-Efficient and Selective Removal of Cationic Dyes from Wastewater Using Hollow Polydopamine Microcapsules: Isotherm, Kinetics, Thermodynamics and Mechanism, *Applied Surface Science*, **542:** 148633 (2021).

[54] Sabarish R., Unnikrishnan G., Polyvinyl Alcohol/Carboxymethyl Cellulose/Zsm-5 Zeolite Biocomposite Membranes for Dye Adsorption Applications, *Carbohydrate Polymers*, **199:** 129-140 (2018).

[55] Jayasantha Kumari H., Krishnamoorthy P., Arumugam T.K., Radhakrishnan S., Vasudevan D., An Efficient Removal of Crystal Violet Dye from Waste Water by Adsorption onto Tlac/Chitosan Composite: A Novel Low Cost Adsorbent, *International Journal of Biological Macromolecules*, **96:** 324-333 (2017).

[56] Duraipandian J., Rengasamy T., Vadivelu S., Experimental and Modeling Studies for the Removal of Crystal Violet Dye from Aqueous Solutions Using Eco-Friendly Gracilaria Corticata Seaweed Activated Carbon/Zn/Alginate Polymeric Composite Beads, *J. Poly. Envir.*, **25(4):** 1062-1071 (2017).

[57] Shirsath S.R., Patil A.P., Bhanvase B.A., Sonawane S.H., Ultrasonically Prepared Poly(Acrylamide)-Kaolin Composite Hydrogel for Removal of Crystal Violet Dye from Wastewater, *J. Envir. Chem. Eng.*, **3(2):** 1152-1162 (2015).

[58] Parab H., Sudersanan M., Shenoy N., Pathare T., Vaze B., Use of Agro-Industrial Wastes for Removal of Basic Dyes from Aqueous Solutions, *CLEAN–Soil, Air, Water*, **37(12):** 963-969 (2009).

[59] Gandhimathi R., Ramesh S.T., Sindhu V., Nidheesh P.V., Bottom Ash Adsorption of Basic Dyes from Their Binary Aqueous Solutions, *Songklanakarin Journal of Science & Technology*, **35(3):** (2013).

[60] Nayl A., Abd-Elhamid A., Abu-Saied M., El-Shanshory A.A., Soliman H.M., Akl M.A., Aly H., A Novel Method for Highly Effective Removal and Determination of Binary Cationic Dyes in Aqueous Media Using a Cotton–Graphene Oxide Composite, *RSC Advances*, **10(13):** 7791-7802 (2020).

[61] Esmaeili H., Foroutan R., Adsorptive Behavior of Methylene Blue onto Sawdust of Sour Lemon, Date Palm, and Eucalyptus as Agricultural Wastes, *J. Dis. Sci. Tech.*, **40(7):** 990-999 (2018).

[62] Noori M., Tahmasebpoor M., Foroutan R., Enhanced Adsorption Capacity of Low-Cost Magnetic Clinoptilolite Powders/Beads for the Effective Removal of Methylene Blue: Adsorption and Desorption Studies, *Materials Chemistry and Physics*, **278:** 125655 (2022).

[63] Wang Y., Zhang Y., Li S., Zhong W., Wei W., Enhanced Methylene Blue Adsorption onto Activated Reed-Derived Biochar by Tannic Acid, *Journal of Molecular Liquids*, **268:** 658-666 (2018).

[64] Khan N.A., Najam T., Shah S.S.A., Hussain E., Ali H., Hussain S., Shaheen A., Ahmad K., Ashfaq M., Development of Mn-Pba on Go Sheets for Adsorptive Removal of Ciprofloxacin from Water: Kinetics, Isothermal, Thermodynamic and Mechanistic Studies, *Materials Chemistry and Physics*, **245:** 122737 (2020).

[65] Somsesta N., Sricharoenchaikul V., Aht-Ong D., Adsorption Removal of Methylene Blue onto Activated Carbon/Cellulose Biocomposite Films: Equilibrium and Kinetic Studies, *Materials Chemistry and Physics*, **240:** 122221 (2020).

[66] Foroutan R., Peighambardoust S.J., Hemmati S., Khatooni H., Ramavandi B., Preparation of Clinoptilolite/Starch/$CoFe_2O_4$ Magnetic Nanocomposite Powder and Its Elimination Properties for Cationic Dyes from Water and Wastewater, *International Journal of Biological Macromolecules*, **189:** 432-442 (2021).

[67] Mahdavinia G.R., Soleymani M., Sabzi M., Azimi H., Atlasi Z., Novel Magnetic Polyvinyl Alcohol/Laponite RD Nanocomposite Hydrogels for Efficient Removal of Methylene Blue, *Journal of environmental chemical engineering*, **5(3):** 2617-2630 (2017).

[68] Mahdavinia G.R., Aghaie H., Sheykhloie H., Vardini M.T., Etemadi H., Synthesis of Caralg/Mmt Nanocomposite Hydrogels and Adsorption of Cationic Crystal Violet, *Carbohydrate Polymers*, **98(1):** 358-365 (2013).

[69] Pandey L.M., Enhanced Adsorption Capacity of Designed Bentonite and Alginate Beads for the Effective Removal of Methylene Blue, *Applied Clay Science*, **169:** 102-111 (2019).

[70] Fan S., Wang Y., Wang Z., Tang J., Tang J., Li X., Removal of Methylene Blue from Aqueous Solution by Sewage Sludge-Derived Biochar: Adsorption Kinetics, Equilibrium, Thermodynamics and Mechanism, *Journal of Environmental Chemical Engineering*, **5(1):** 601-611 (2017).

[71] Haldar D., Duarah P., Purkait M.K., Mofs for the Treatment of Arsenic, Fluoride and Iron Contaminated Drinking Water: A Review, *Chemosphere*, **251:** 126388 (2020).

[72] Kumar M., Puri A., A Review of Permissible Limits of Drinking Water, *Indian Journal of Occupational and Environmental Medicine*, **16(1):** 40 (2012).